

Politecnico
di Torino

Politecnico di Torino

Corso di Laurea Magistrale
in Ingegneria dell'Autoveicolo

Path Tracking Control for Automated Vehicles Operating at the Limit of Handling

Candidate

Noel Edwin D'Cruz

Supervisors

Prof. Aldo Sorniotti, Cecilia Formento, Salvatore Ingraffia

DIMEAS – Dipartimento di Ingegneria Meccanica e Aerospaziale

Academic Year 2025–2026

Abstract

Automated vehicles must maintain accurate path tracking and vehicle stability even when operating close to the physical limits of handling. Under these conditions, the nonlinear behaviour of vehicle dynamics and tyre-road interactions can challenge conventional control approaches, particularly during active safety manoeuvres requiring rapid steering and braking actions.

This thesis investigates the application of Nonlinear Model Predictive Control (NMPC) for path tracking control of automated vehicles operating near the handling limits. The proposed control framework is implemented using the ACADOS optimization framework and integrated within a MATLAB/Simulink environment to enable computationally efficient real-time optimization. A nonlinear vehicle model including longitudinal, lateral, yaw, and wheel rotational dynamics is employed within the prediction model to represent vehicle behaviour under demanding driving conditions.

The control architecture exploits integrated steering and braking actions to achieve trajectory tracking, vehicle stabilization, and speed regulation. The optimization problem minimizes path tracking errors, heading errors, speed tracking errors, and control effort while respecting vehicle and actuator constraints. Particular attention is devoted to controller tuning, prediction horizon design, and constraint formulation to ensure stable operation at increasing vehicle speeds.

The framework is evaluated through simulation studies representative of active safety applications, including high-speed path-following and emergency manoeuvres requiring simultaneous trajectory tracking and vehicle deceleration. The analysis focuses on the controller's ability to maintain stability and tracking performance while operating near the vehicle's handling limits.

The results demonstrate the potential of NMPC as an effective control strategy for high-performance automated driving applications. Furthermore, the proposed framework establishes a foundation for future developments involving adaptive and learning-based control techniques, enabling the integration of artificial intelligence methods with model-based predictive control to further enhance vehicle performance and safety.

Acknowledgment

Firstly, I would like to thank Prof. Aldo Sorniotti for providing this amazing opportunity, and Cecilia Formento and Salvatore Ingraffia for their constant support and for mentoring me throughout my thesis. Without their constant support, it would not have been possible to learn so much. Thank you for your guidance, which gave me confidence that I would thrive not only academically but also professionally. I really appreciate your time with me.

I thank my parents for their belief in me and for giving me the opportunity to do what I want to do, and I will always be grateful for that freedom and support. Thank you Kevin for always believing in me, whenever I doubt myself.

My utmost thanks to Abhishek Samanta for teaching me everything and guiding me properly, which led me to complete my master's sooner than I expected; indeed, you are a great teacher. Thank you so much. Finally, to my two best friends, Sunidhi Gemawat and Jeet Patel, for checking on me constantly and making me feel like you are always beside me no matter what. Thank you all.

Contents

1 Chapter 1: Introduction **8**
- 1.1 Literature Review . . . 9
  - 1.1.1 Automated Vehicle Path Tracking . . . 9
  - 1.1.2 Path Tracking Performance Metrics . . . 10
  - 1.1.3 Vehicle Dynamics Near the Handling Limits . . . 12
  - 1.1.4 Conventional Path Tracking Controllers . . . 14
  - 1.1.5 Model Predictive Control . . . 15
  - 1.1.6 Nonlinear Model Predictive Control . . . 17
  - 1.1.7 Research Gap and Thesis Objectives . . . 19

2 NMPC Internal Model Description and Validation **21**
- 2.1 Introduction . . . 21
- 2.2 Vehicle Modeling Approach . . . 21
- 2.3 Nonlinear Four-Wheel Vehicle Model . . . 23
- 2.4 Tyre Force and Load Transfer Modeling . . . 26
  - 2.4.1 Pacejka-Based tyre Model . . . 26
  - 2.4.2 Combined Slip Effects . . . 26
  - 2.4.3 Rolling Resistance Moment . . . 27
  - 2.4.4 Dynamic Load Transfer . . . 27
- 2.5 Vehicle Equations of Motion . . . 29
  - 2.5.1 Translational Dynamics . . . 29
  - 2.5.2 Yaw Dynamics . . . 30
  - 2.5.3 Wheel Rotational Dynamics . . . 31
- 2.6 Steering and Brake Actuator Dynamics . . . 32

3 Optimal Control Problem Formulation and Assumptions **34**
- 3.1 Introduction . . . 34
- 3.2 NMPC Problem Formulation . . . 35
- 3.3 Cost Function Design . . . 36
- 3.4 Constraints . . . 38
  - 3.4.1 State Constraints . . . 38

3.4.2 Input Constraints . . . 39
3.4.3 Soft Constraints and Slack Variables . . . 39
3.5 Prediction Horizon and Discretization . . . 40
3.6 ACADOS Solver Configuration . . . 42
3.6.1 Nonlinear Programming Solver . . . 42
3.6.2 Quadratic Programming Solver . . . 43
3.6.3 Numerical Integration Method . . . 43
3.6.4 Globalization Strategy . . . 43
3.6.5 Warm Starting . . . 44
3.6.6 Regularization Strategy . . . 44
3.6.7 Solver Tolerances . . . 44

4 Simulation Environment and Results 46
4.1 Introduction . . . 46
4.2 Emergency Evasive Manoeuvre . . . 46
4.2.1 Reference Path Design . . . 47
4.2.2 Vehicle Initial Conditions . . . 48
4.2.3 Tested Vehicle Speeds . . . 48
4.3 Path Tracking Performance . . . 49
4.3.1 Vehicle Trajectory Tracking . . . 49
4.3.2 Cross-Track and Heading Error Analysis . . . 49
4.4 Vehicle Dynamic Response . . . 52
4.4.1 Velocity, Lateral Acceleration and Sideslip Angle Response . . . 53
4.4.2 Steering and Braking Actions . . . 53
4.5 Constraint Satisfaction . . . 60
4.6 Tyre Slip Behaviour . . . 62
4.7 NMPC Prediction Behaviour . . . 63
4.7.1 Predicted Vehicle States . . . 64
4.7.2 Predicted Wheel Rotational Speeds . . . 64
4.7.3 Predicted Control Inputs . . . 67
4.8 Constraint Satisfaction and Solver Performance . . . 67
4.9 Chapter Summary . . . 69

5 Conclusions and Future Work 71
5.1 Conclusions . . . 71
5.2 Main Contributions . . . 72
5.3 Limitations . . . 73
5.4 Future Research Directions . . . 74

List of Figures

1.1 General architecture of an autonomous driving system showing the relationship between perception, planning, and vehicle control functions. 8
1.2 Path Tracking within the Autonomous Driving Architecture. . 9
1.3 Typical path tracking problem illustrating the cross-track error (e_y) and heading error (e_ψ) between the reference trajectory and the actual vehicle motion. 11
1.4 Friction circle illustrating the trade-off between longitudinal force (F_x) and lateral force (F_y) under limited tyre-road adhesion. 12
1.5 Basic operating principle of Model Predictive Control (MPC). 16
1.6 Non-Linear Model Predictive Control (NMPC). 17

2.1 Comparison of common vehicle modeling approaches used for vehicle control applications. 22
2.2 Schematic representation of the nonlinear four-wheel vehicle model including vehicle states, steering angles, and tyre force components. 25
2.3 Illustration of longitudinal and lateral load transfer effects during acceleration, braking, and cornering manoeuvres. 28
2.4 Longitudinal and lateral force components acting on the vehicle body-fixed reference frame. 30

3.1 Receding horizon implementation of the NMPC framework adopted in this work. 35
3.2 Components of the NMPC cost function used in the optimization problem. 38
3.3 Soft longitudinal slip constraints imposed on each wheel within the NMPC formulation. 40
3.4 Non-uniform prediction horizon discretization adopted in the NMPC formulation. 41

4.1 Reference evasive manoeuvre trajectory used for controller evaluation. 47
4.2 Vehicle trajectory tracking performance during the evasive manoeuvre at different initial vehicle speeds. 50
4.3 Vehicle trajectory tracking performance during the evasive manoeuvre at different initial vehicle speeds. 51
4.4 Vehicle speed, lateral acceleration and sideslip angle responses during the emergency steering manoeuvre for initial vehicle speeds 60km/hr. 54
4.5 Vehicle speed, lateral acceleration and sideslip angle responses during the emergency steering manoeuvre for initial vehicle speeds 65km/hr. 55
4.6 Vehicle speed, lateral acceleration and sideslip angle responses during the emergency steering manoeuvre for initial vehicle speeds 70km/hr. 56
4.7 Steering angles and braking responses during the emergency manoeuvre manoeuvre for initial vehicle speeds 60km/hr. . . . 57
4.8 Steering angles and braking responses during the emergency manoeuvre manoeuvre for initial vehicle speeds 65km/hr. . . . 58
4.9 Steering angles and braking responses during the emergency manoeuvre manoeuvre for initial vehicle speeds 70km/hr. . . . 59
4.10 Constraint violation map for all constrained states during the evasive manoeuvre. A value of zero indicates that all constraints are satisfied. 61
4.11 Tyre slip behaviour at 60km/hr. 62
4.12 Tyre slip behaviour at 65km/hr. 62
4.13 Tyre slip behaviour at 70km/hr. 63
4.14 Prediction Vehicle States at different initial speeds. 65
4.15 Prediction Wheel Rotation at different initial speeds. 66
4.16 Prediction Control Inputs at different initial speeds. 68

List of Tables

1.1 Common path tracking performance metrics. 11
1.2 Comparison of conventional path tracking controllers. 15
1.3 Main characteristics of Model Predictive Control. 17

2.1 State variables of the nonlinear vehicle model. 24

3.1 State constraints used in the NMPC formulation. 39
3.2 Input constraints used in the NMPC formulation. 39
3.3 ACADOS solver tolerances. 44

Chapter 1

Chapter 1: Introduction

Autonomous vehicles have attracted significant attention in recent years due to their potential to improve road safety, traffic efficiency, and driving comfort. Advances in sensing technologies, computational capabilities, and control systems have enabled vehicles to perform increasingly complex driving tasks with reduced human intervention.

One of the fundamental functions of an autonomous vehicle is *path tracking*, which consists of accurately following a desired trajectory generated by the planning system. As shown in Figure 1.1, the control layer is responsible for converting the planned trajectory into steering, braking, and propulsion commands that guide the vehicle along the desired path.

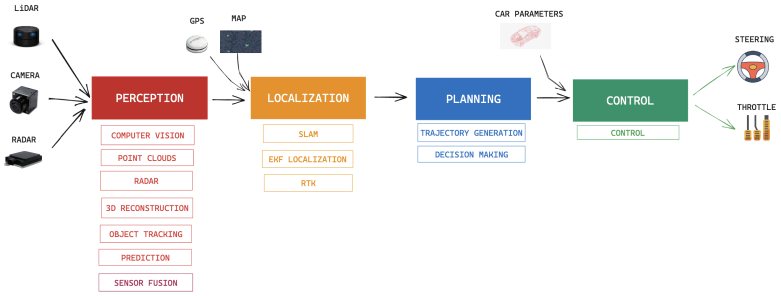


Figure 1.1: General architecture of an autonomous driving system showing the relationship between perception, planning, and vehicle control functions.

While path tracking can be achieved relatively easily during normal driving conditions, it becomes significantly more challenging when the vehicle operates near its handling limits. During aggressive manoeuvres such as emergency obstacle avoidance, rapid lane changes, or high-speed cornering, tyre forces approach saturation and vehicle dynamics become strongly nonlin-

ear. Under these conditions, maintaining accurate trajectory tracking while preserving vehicle stability represents a demanding control problem.

To address these challenges, this thesis investigates the application of Nonlinear Model Predictive Control (NMPC) for automated vehicle path tracking near the handling limits. The proposed approach aims to improve trajectory tracking performance by explicitly considering nonlinear vehicle dynamics and system constraints within an optimization-based control framework.

1.1 Literature Review

1.1.1 Automated Vehicle Path Tracking

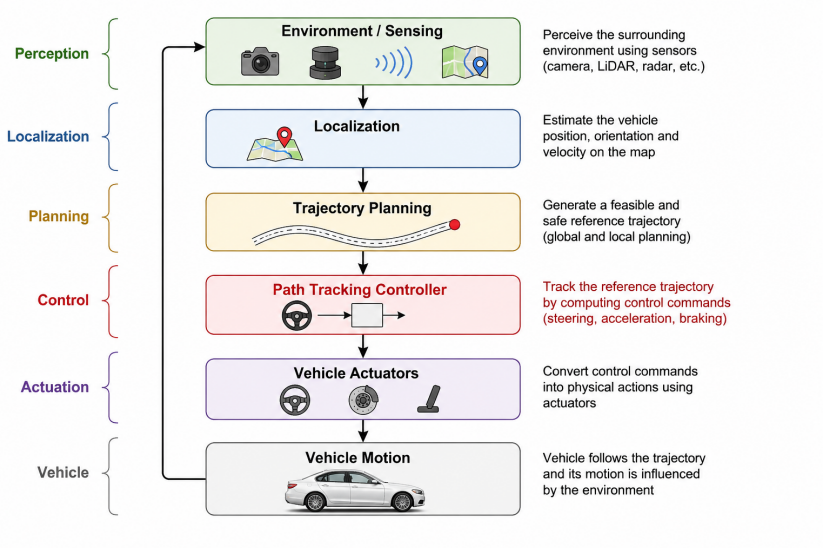


Figure 1.2: Path Tracking within the Autonomous Driving Architecture.

Path tracking is one of the fundamental functions of an autonomous vehicle control system. Its objective is to ensure that the vehicle accurately follows a reference trajectory generated by the motion planning layer while maintaining stability, safety, and passenger comfort. As illustrated in Figure 1.2, path tracking acts as the interface between trajectory planning and vehicle actuation, converting the desired path into steering, braking, and propulsion commands.

The importance of path tracking has increased considerably with the development of highly automated driving systems. Modern autonomous vehicles are expected to operate in a wide range of driving scenarios, including

urban environments, highways, and emergency situations. In all these cases, the controller must continuously compensate for disturbances, modelling uncertainties, and variations in vehicle operating conditions while ensuring accurate trajectory execution.

The path tracking problem is commonly formulated as the minimization of the deviation between the reference trajectory and the actual vehicle motion. This requires the controller to continuously evaluate the vehicle state and determine appropriate control actions capable of reducing tracking errors while respecting vehicle and actuator limitations. The resulting control actions directly influence the vehicle behaviour and therefore play a critical role in overall autonomous driving performance.

As vehicle speeds increase and driving manoeuvres become more demanding, the path tracking problem becomes increasingly challenging due to the nonlinear characteristics of vehicle dynamics and tyre-road interactions. Consequently, significant research efforts have focused on developing advanced path tracking controllers capable of maintaining high tracking accuracy while preserving vehicle stability under challenging operating conditions.

1.1.2 Path Tracking Performance Metrics

The objective of a path tracking controller is to minimize the deviation between the desired trajectory and the actual vehicle motion. To evaluate controller performance, several tracking metrics are commonly employed in the literature. These metrics quantify the accuracy with which the vehicle follows the reference path while maintaining stable and safe operation.

Among the most widely used performance indicators are the cross-track error and the heading error, illustrated in Figure 1.3. The cross-track error represents the lateral distance between the vehicle and the reference trajectory, while the heading error describes the difference between the vehicle orientation and the desired trajectory direction. Together, these variables provide a direct measure of path tracking accuracy and are frequently incorporated into the controller objective function.

In addition to lateral tracking performance, autonomous vehicle controllers must also regulate the vehicle speed according to the driving scenario. Consequently, the longitudinal velocity error is often considered as an additional performance metric, particularly during emergency manoeuvres or highly dynamic driving conditions where simultaneous steering and speed control are required.

The performance objectives summarized in Table 1.1 are often conflicting. For example, aggressive steering actions may reduce tracking errors but can negatively affect vehicle stability and passenger comfort. Therefore, an ef-

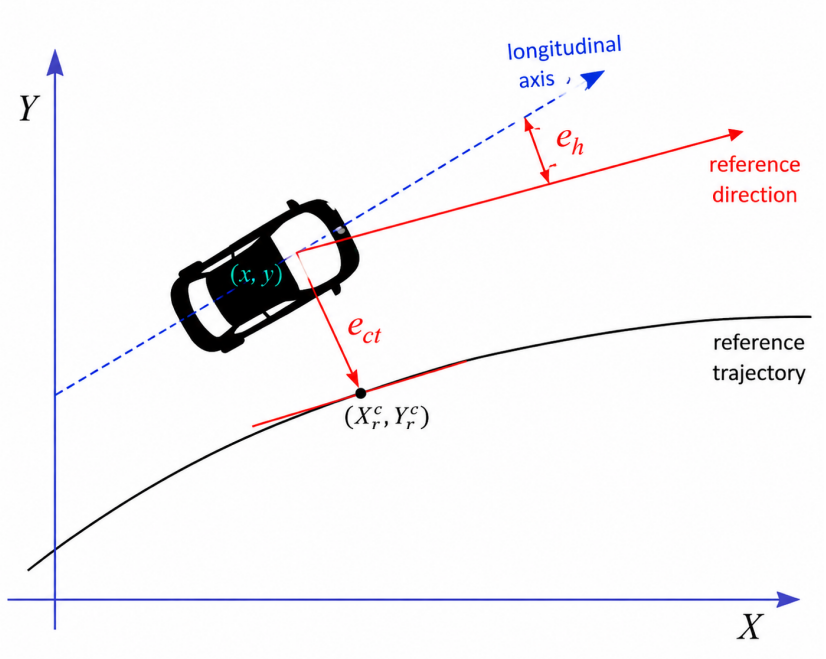


Figure 1.3: Typical path tracking problem illustrating the cross-track error (e_y) and heading error (e_ψ) between the reference trajectory and the actual vehicle motion.

Table 1.1: Common path tracking performance metrics.

Metric	Description
Cross-track error (e_y)	Lateral distance between the vehicle and the reference path
Heading error (e_ψ)	Difference between vehicle heading and reference heading
Velocity error	Difference between actual and desired vehicle speed
Steering effort	Magnitude of steering control action
Passenger comfort	Smoothness of vehicle motion and control inputs

fective path tracking controller must achieve a compromise between tracking accuracy, vehicle stability, control effort, and overall safety.

1.1.3 Vehicle Dynamics Near the Handling Limits

The performance of a path tracking controller is strongly influenced by the dynamic behaviour of the vehicle. During normal driving conditions, tyre forces generally remain within a nearly linear operating region, allowing simplified vehicle models and conventional control strategies to achieve satisfactory tracking performance. However, during aggressive manoeuvres such as emergency obstacle avoidance, rapid lane changes, and high-speed cornering, the vehicle may operate close to its physical handling limits. Under these conditions, tyre forces approach saturation, vehicle dynamics become highly nonlinear, and maintaining stable path tracking becomes significantly more challenging [1, 2].

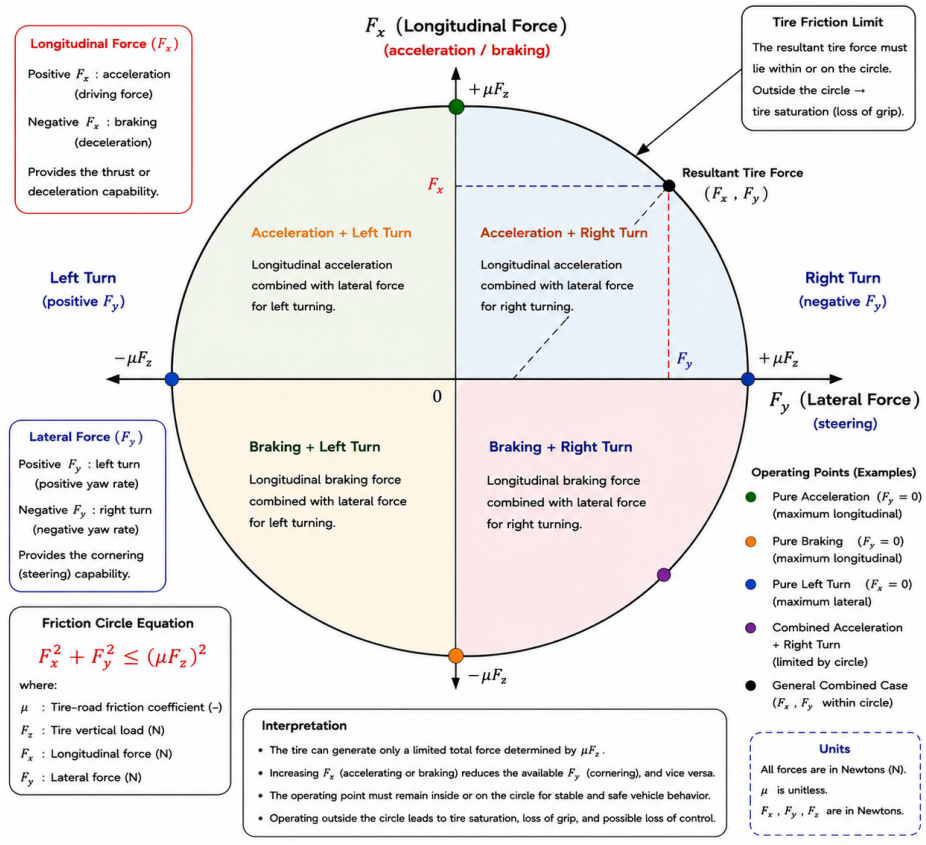


Figure 1.4: Friction circle illustrating the trade-off between longitudinal force (F_x) and lateral force (F_y) under limited tyre-road adhesion.

A fundamental factor governing vehicle behaviour near the handling limits is the limited tyre-road friction available for force generation. As illustrated by the friction circle shown in Figure 1.4, the tyre must simultaneously generate longitudinal forces for acceleration or braking and lateral forces for steering. These forces are constrained by the available friction between the tyre and the road surface, resulting in a trade-off between longitudinal and lateral force generation. Consequently, increasing braking or acceleration effort reduces the amount of lateral force available for cornering, and vice versa.

The significance of this force coupling becomes particularly evident when the vehicle approaches the friction limits of the tyres. Funke et al. demonstrated that emergency collision avoidance manoeuvres often require autonomous vehicles to operate close to the handling limits and exploit a large portion of the available tyre force envelope rather than remaining within conservative linear operating regions [1]. Their experimental results showed that incorporating tyre nonlinearities allows the controller to utilize the full performance capability of the vehicle during critical manoeuvres.

As tyre saturation increases, the relationship between tyre slip and force generation becomes strongly nonlinear. Weber and Gerdes highlighted that drifting and limit-handling manoeuvres activate dynamic effects such as wheel-speed dynamics, load transfer, and tyre saturation, all of which significantly influence the forces acting on the vehicle [2]. Similarly, Goh et al. demonstrated that operation beyond conventional stability boundaries requires explicit consideration of coupled longitudinal and lateral tyre slip within the predictive control formulation [3]. Their results showed that simplified decoupled tyre models may become inadequate when tyres operate in highly saturated conditions.

In addition to tyre saturation, vehicle handling is influenced by load transfer effects caused by acceleration, braking, and cornering. Variations in vertical tyre load alter the available friction force at each wheel and therefore modify the overall vehicle response. These effects become increasingly significant as vehicle speed increases and the available time for corrective control actions decreases.

Consequently, maintaining accurate trajectory tracking near the handling limits requires controllers capable of accounting for nonlinear tyre behaviour, force saturation, and physical actuator constraints. These challenges have motivated the development of advanced predictive control approaches, particularly Nonlinear Model Predictive Control (NMPC), which can incorporate nonlinear vehicle dynamics and constraints directly within the optimization process.

1.1.4 Conventional Path Tracking Controllers

Over the past decades, numerous control strategies have been proposed to address the path tracking problem in autonomous vehicles. These approaches differ in complexity, computational requirements, and their ability to handle nonlinear vehicle dynamics and operational constraints.

Among the earliest solutions, Proportional-Integral-Derivative (PID) controllers have been widely used due to their simplicity and ease of implementation. PID controllers generate steering commands based on the current tracking error and its variation over time. While they can provide satisfactory performance under moderate operating conditions, their effectiveness decreases when vehicle dynamics become strongly nonlinear or when significant disturbances are present.

Geometric controllers such as Pure Pursuit and the Stanley controller were later introduced to improve path tracking performance. Pure Pursuit determines the steering command by continuously targeting a look-ahead point located on the reference trajectory. The Stanley controller combines heading and lateral tracking errors to improve convergence towards the desired path. Both approaches have demonstrated good performance in practical applications and have been successfully implemented in autonomous vehicle platforms. However, their performance may deteriorate during highly dynamic manoeuvres where tyre saturation and vehicle nonlinearities become significant.

Linear Quadratic Regulator (LQR) controllers represent a more systematic control approach based on state-space modelling and optimal control theory. By minimizing a quadratic cost function, LQR controllers provide improved tracking performance compared to purely geometric methods. Nevertheless, their effectiveness relies on linearized vehicle models and may therefore be limited when the vehicle operates near the handling limits. [4, 5]

The limitations of conventional controllers become increasingly apparent during aggressive manoeuvres that involve strong nonlinearities, tyre force saturation, and actuator constraints. Under such conditions, simplified control laws may not adequately capture the true vehicle behaviour, potentially leading to reduced tracking accuracy and degraded stability. These challenges have motivated the development of advanced predictive control techniques capable of explicitly accounting for system dynamics and physical constraints.

Table 1.2 summarizes the main characteristics, advantages, and limitations of the most common path tracking control approaches. The controllers presented in Table 1.2 have contributed significantly to the advancement of autonomous vehicle technology and remain widely used in industrial and

Table 1.2: Comparison of conventional path tracking controllers.

Controller	Advantages	Limitations
PID	Simple implementation and low computational cost	Limited performance under nonlinear conditions
Pure Pursuit	Easy implementation and intuitive geometric formulation	Reduced accuracy during aggressive manoeuvres
Stanley	Good path convergence and practical applicability	Sensitive to parameter tuning at high speed
LQR	Optimal control formulation and improved tracking performance	Relies on linearized vehicle models

academic applications. Nevertheless, their ability to handle highly nonlinear vehicle dynamics and explicitly incorporate system constraints is limited. As a result, increasing research attention has shifted towards Model Predictive Control (MPC), which offers a unified framework for trajectory tracking, constraint handling, and optimal control.

1.1.5 Model Predictive Control

Model Predictive Control (MPC) has emerged as one of the most successful advanced control strategies for autonomous vehicle applications due to its ability to explicitly account for system dynamics and operational constraints. Unlike conventional feedback controllers, MPC predicts the future behaviour of the system over a finite prediction horizon and computes the control actions that optimize a predefined performance criterion.

The basic operating principle of MPC is illustrated in Figure 1.5. At each sampling instant, a mathematical model of the vehicle is used to predict future system behaviour over a specified prediction horizon. An optimization problem is then solved to determine the sequence of control inputs that minimizes a cost function while satisfying system constraints. Only the first control action of the optimized sequence is applied to the vehicle, after which the optimization process is repeated using updated state measurements.

One of the primary advantages of MPC is its ability to incorporate mul-

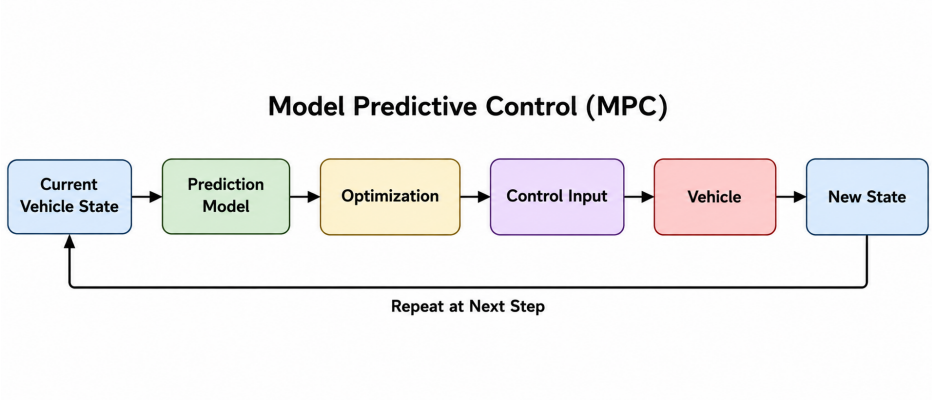


Figure 1.5: Basic operating principle of Model Predictive Control (MPC).

tiple control objectives within a unified optimization framework. For vehicle path tracking applications, the cost function typically penalizes tracking errors, control effort, and variations in actuator commands. At the same time, physical constraints such as steering limits, acceleration limits, and safety-related requirements can be directly enforced within the optimization problem.[6]

Several studies have demonstrated the effectiveness of MPC for autonomous vehicle control, particularly in scenarios involving obstacle avoidance, trajectory tracking, and vehicle stabilization. Compared to conventional controllers, MPC offers improved flexibility and a systematic framework for balancing competing objectives while respecting system limitations.

Despite these advantages, the performance of MPC strongly depends on the accuracy of the prediction model. When linear prediction models are employed, prediction accuracy may deteriorate under highly dynamic operating conditions where vehicle nonlinearities become significant. Consequently, the use of nonlinear prediction models has received increasing attention in recent years, leading to the development of Nonlinear Model Predictive Control (NMPC) approaches specifically designed for operation near the vehicle handling limits.

The features summarized in Table 1.3 have contributed to the widespread adoption of MPC in autonomous driving research. In particular, the ability to simultaneously consider trajectory tracking objectives and actuator constraints makes MPC well suited for vehicle control applications. However, the reliability of simplified prediction models remains a limitation when operating near the handling limits, where nonlinear vehicle behaviour becomes dominant.[5]

Table 1.3: Main characteristics of Model Predictive Control.

Characteristic	Description
Prediction Horizon	Predicts future system behaviour over a finite time interval
Optimization-Based	Computes control inputs by solving an optimization problem
Constraint Handling	Explicitly incorporates physical and operational constraints
Multi-Objective Capability	Simultaneously considers multiple performance objectives

1.1.6 Nonlinear Model Predictive Control

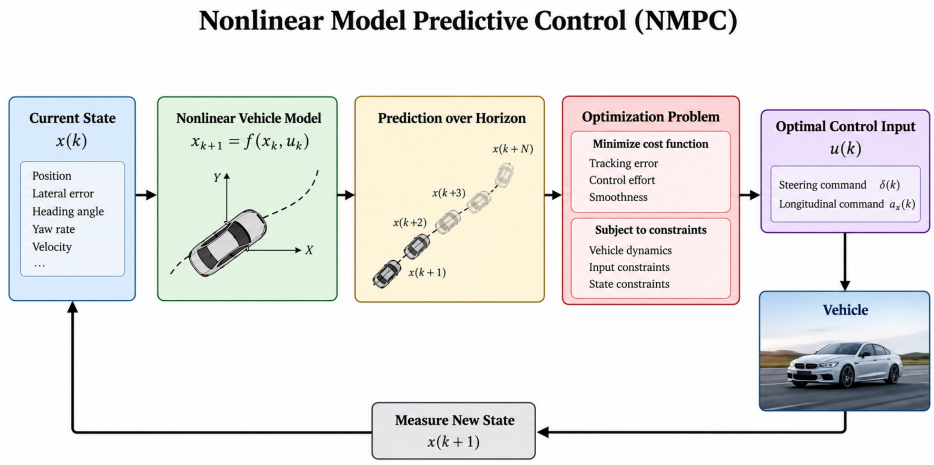


Figure 1.6: Non-Linear Model Predictive Control (NMPC).

The effectiveness of Model Predictive Control depends strongly on the accuracy of the prediction model used within the optimization process. While linear prediction models can provide satisfactory performance under moderate operating conditions, their accuracy deteriorates when the vehicle approaches its handling limits, where tyre saturation, load transfer, and nonlinear tyre-road interactions become dominant. Under these conditions, the simplifying assumptions adopted in linear vehicle models may no longer accurately represent the true vehicle behaviour.

To address these limitations, Nonlinear Model Predictive Control (NMPC) extends the conventional MPC framework by incorporating nonlinear system dynamics directly within the prediction model. As illustrated in Figure 1.6, the controller predicts future vehicle behaviour using a nonlinear vehicle

model and computes the optimal control inputs by solving a constrained optimization problem at each sampling instant. This approach enables a more accurate representation of vehicle dynamics during highly aggressive manoeuvres while preserving the ability to explicitly handle physical and safety-related constraints.

The capability of NMPC to account for nonlinear vehicle behaviour has made it particularly attractive for autonomous driving applications involving operation near the handling limits. Several studies have demonstrated that NMPC can achieve superior tracking performance compared to controllers based on linearized models, especially in situations where tyre saturation and combined-slip effects become significant [1, 3].

Recent research has increasingly focused on the application of NMPC to highly dynamic vehicle manoeuvres. Funke et al. developed a predictive control framework for emergency collision avoidance and stabilization, demonstrating that nonlinear vehicle models allow the controller to exploit a larger portion of the available tyre force envelope while maintaining vehicle stability during critical manoeuvres [1]. Their work highlighted the importance of accurately capturing tyre nonlinearities when operating close to the friction limits.

Weber and Gerdes investigated the modelling and control of dynamic drifting trajectories using NMPC-based techniques capable of handling significant tyre saturation and large vehicle slip angles [2]. Their results demonstrated that advanced predictive controllers can successfully stabilize vehicle motion even when operating beyond the conventional limits associated with normal driving conditions.

Similarly, Goh et al. proposed an NMPC framework for highly transient autonomous drifting, incorporating coupled longitudinal and lateral tyre slip within the prediction model [3]. The authors demonstrated that nonlinear predictive control can maintain accurate vehicle control during aggressive drifting manoeuvres while explicitly accounting for tyre force saturation effects.

Beyond drifting applications, NMPC has also been employed for integrated vehicle dynamics control. Studies combining predictive control with direct yaw moment control and torque vectoring strategies have shown improved stability and trajectory tracking performance during aggressive manoeuvres [7, 8]. These approaches exploit the predictive capabilities of NMPC to coordinate multiple vehicle actuators while respecting physical limitations and safety constraints.

Despite its advantages, NMPC introduces a significantly higher computational burden compared to conventional controllers and linear MPC approaches. The need to repeatedly solve nonlinear optimization problems in

real time represents one of the main challenges associated with practical implementation. However, recent advances in numerical optimization techniques and software frameworks such as CasADi and ACADOS have substantially improved the feasibility of real-time NMPC applications for automotive systems.

As a result, NMPC has emerged as one of the most promising control strategies for autonomous vehicles operating near the handling limits, offering a systematic framework capable of simultaneously addressing trajectory tracking, vehicle stability, actuator constraints, and nonlinear vehicle dynamics.

1.1.7 Research Gap and Thesis Objectives

The literature reviewed in the previous sections demonstrates the significant progress achieved in autonomous vehicle path tracking and vehicle dynamics control. Conventional approaches such as PID, Pure Pursuit, Stanley, and LQR controllers have proven effective under normal driving conditions but often experience performance degradation when the vehicle operates close to its handling limits. To overcome these limitations, Model Predictive Control (MPC) and, more recently, Nonlinear Model Predictive Control (NMPC) have emerged as powerful control frameworks capable of explicitly considering system dynamics and operational constraints.

Recent studies have shown that NMPC can successfully address highly dynamic driving scenarios, including emergency obstacle avoidance, vehicle stabilization, and autonomous drifting manoeuvres. In particular, research conducted by Funke et al. [1], Weber and Gerdes [2], and Goh et al. [3] demonstrated the ability of nonlinear predictive controllers to exploit a larger portion of the available tyre force envelope while maintaining vehicle stability under aggressive operating conditions. Furthermore, integrated control strategies combining NMPC with direct yaw moment control and torque vectoring have shown additional improvements in vehicle handling and safety.

Despite these advances, several challenges remain. Many existing studies focus on highly specialized scenarios such as autonomous drifting or emergency collision avoidance, where the primary objective is vehicle stabilization under extreme conditions. While these investigations provide valuable insights into vehicle behaviour near the handling limits, their control architectures are often tailored to specific manoeuvres and may not directly address the broader path tracking problem encountered in autonomous driving applications.

In addition, the successful implementation of NMPC relies heavily on the selection of an appropriate vehicle model capable of accurately representing

the nonlinear dynamics that dominate near the friction limits. Achieving a balance between model fidelity and computational efficiency remains a fundamental challenge, particularly when real-time implementation requirements are considered.

Motivated by these observations, this thesis investigates the application of Nonlinear Model Predictive Control for vehicle path tracking at the limit of handling. Particular attention is given to the development and validation of a nonlinear vehicle model suitable for predictive control, the formulation of the associated optimal control problem, and the evaluation of controller performance during aggressive manoeuvres representative of high-demand driving scenarios.

The primary objectives of this thesis can be summarized as follows:

- Develop a nonlinear vehicle model capable of capturing the dominant dynamic effects relevant to path tracking near the handling limits.
- Formulate a constrained Nonlinear Model Predictive Control problem suitable for autonomous vehicle trajectory tracking.
- Investigate the ability of the proposed controller to maintain tracking accuracy and vehicle stability during aggressive manoeuvres.
- Evaluate the effectiveness of the proposed approach through simulation studies representative of high-demand driving conditions.

The following chapter presents the nonlinear vehicle model adopted in this work and its validation prior to the development of the predictive control framework.

Chapter 2

NMPC Internal Model Description and Validation

2.1 Introduction

The performance of a Nonlinear Model Predictive Controller is strongly dependent on the accuracy of the prediction model used within the optimization process. Since the controller determines future control actions based on predicted vehicle behaviour, the internal model must provide a sufficiently accurate representation of the vehicle dynamics while remaining computationally efficient for real-time implementation.

When operating near the handling limits, simplified vehicle models may fail to capture important nonlinear phenomena such as tyre force saturation, load transfer, and actuator dynamics. These effects can significantly influence vehicle behaviour during aggressive manoeuvres and therefore must be adequately represented within the prediction model.

This chapter presents the nonlinear vehicle model adopted in this work for the development of the NMPC controller. The modeling approach is first introduced, followed by a detailed description of the vehicle dynamics, tyre force formulation, and actuator dynamics incorporated in the model. Finally, the model parameters and validation procedure are presented to assess the suitability of the prediction model for path tracking applications near the handling limits.

2.2 Vehicle Modeling Approach

The selection of an appropriate vehicle model represents a fundamental step in the design of a Nonlinear Model Predictive Controller. The prediction

model must accurately reproduce the dominant vehicle dynamics that influence path tracking performance while maintaining a level of complexity compatible with real-time optimization.

Several vehicle modeling approaches are commonly employed in the literature. Kinematic vehicle models are widely used for low-speed applications due to their simplicity and low computational requirements. However, they neglect tyre forces and inertial effects, making them unsuitable for manoeuvres involving significant lateral accelerations or operation near the vehicle handling limits.

Dynamic bicycle models provide a more realistic representation of vehicle behaviour by incorporating lateral tyre forces, vehicle inertia, and yaw dynamics. These models have been extensively adopted in vehicle control research because they offer a reasonable compromise between accuracy and computational efficiency. Nevertheless, their simplified representation of tyre-road interactions and axle dynamics may limit their accuracy during highly aggressive manoeuvres where tyre saturation, load transfer, and wheel dynamics become significant. [4]

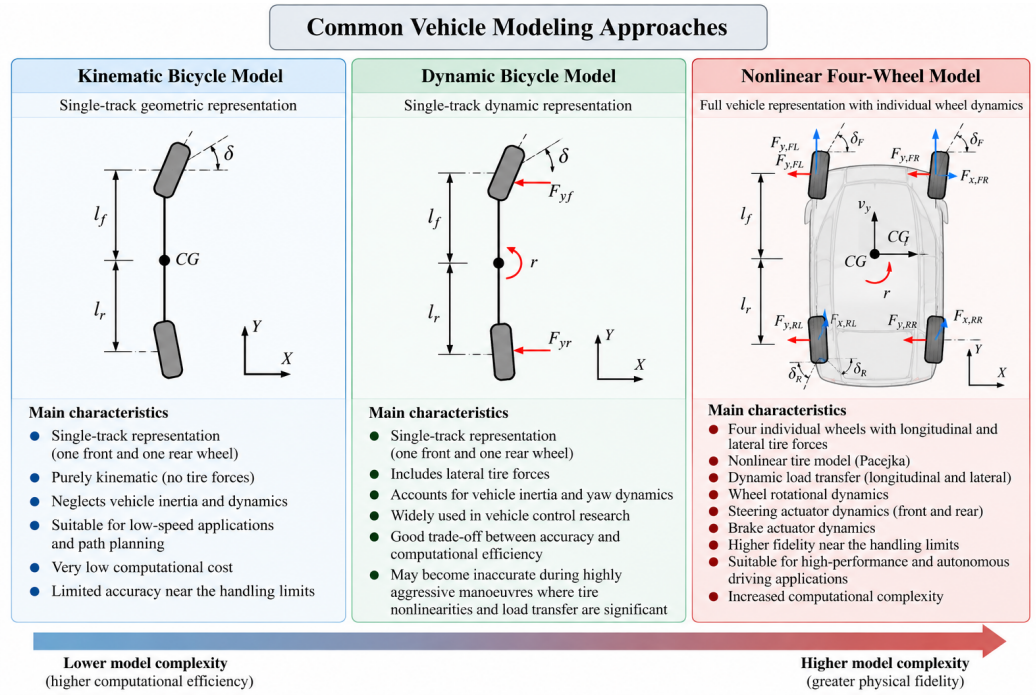


Figure 2.1: Comparison of common vehicle modeling approaches used for vehicle control applications.

Since the objective of this thesis is to investigate path tracking performance near the handling limits, a more detailed nonlinear vehicle model was

adopted. The implemented model represents the vehicle using a four-wheel formulation in which the longitudinal and lateral tyre forces are computed individually for each wheel. In addition, the model incorporates wheel rotational dynamics, steering actuator dynamics, brake actuator dynamics, and dynamic load transfer effects. These features enable a more accurate representation of the nonlinear phenomena that become dominant during aggressive driving conditions.

The resulting model provides a suitable compromise between physical fidelity and computational tractability for nonlinear predictive control applications. By capturing the most relevant dynamic effects while remaining compatible with real-time optimization, the model forms the foundation of the NMPC framework developed in this work.[3]

2.3 Nonlinear Four-Wheel Vehicle Model

To accurately represent vehicle behaviour during aggressive manoeuvres, a nonlinear four-wheel vehicle model was adopted as the prediction model within the NMPC framework. Compared to simplified single-track models, the selected formulation allows the dynamics of each wheel to be represented individually, enabling a more accurate description of tyre-road interactions, wheel rotational behaviour, load transfer effects, and actuator dynamics.

The model considers the vehicle motion in the horizontal plane and describes the translational and rotational dynamics of the vehicle body together with the rotational dynamics of the individual wheels. In addition, steering actuator dynamics and braking actuator dynamics are incorporated to account for the response characteristics of the physical actuators.

Two reference frames are employed in the model formulation. An inertial reference frame (X, Y) is used to describe the global vehicle position, while a body-fixed reference frame (x, y) is attached to the vehicle centre of gravity (CG). The vehicle orientation with respect to the inertial frame is defined by the yaw angle ψ, while the vehicle rotational motion is characterized by the yaw rate r.

The vehicle geometry is defined by the distances between the centre of gravity and the front and rear axles, denoted by l_f and l_r, respectively. Independent steering angles are considered for the front and rear axles, allowing the model to represent both front-wheel and rear-wheel steering effects. Longitudinal and lateral tyre forces are calculated individually at each wheel, resulting in a detailed representation of vehicle dynamics near the handling limits. All details are shown in figure:2.2

The complete state vector adopted in this work is composed of thirteen

states and is expressed as

$$\mathbf{x} = \begin{bmatrix} X \\ Y \\ \psi \\ V_x \\ V_y \\ r \\ \omega_{FL} \\ \omega_{FR} \\ \omega_{RL} \\ \omega_{RR} \\ \delta_F \\ \delta_R \\ T_b \end{bmatrix} \tag{2.1}$$

Table 2.1: State variables of the nonlinear vehicle model.

State	Symbol	Description
Global position	X, Y	Vehicle position in inertial frame
Yaw angle	ψ	Vehicle heading angle
Longitudinal velocity	V_x	Velocity along body x-axis
Lateral velocity	V_y	Velocity along body y-axis
Yaw rate	r	Angular velocity about vertical axis
Wheel speeds	$\omega_{FL}, \omega_{FR}, \omega_{RL}, \omega_{RR}$	Individual wheel angular velocities
Front steering angle	δ_F	Actual front steering angle
Rear steering angle	δ_R	Actual rear steering angle
Brake torque	T_b	Actual brake torque state

The control inputs of the model are defined as the commanded front steering angle, commanded rear steering angle, and commanded brake torque. The input vector is expressed as:

$$\mathbf{u} = \begin{bmatrix} D_F & D_R & T_{brake} \end{bmatrix}^T \tag{2.2}$$

where D_F and D_R represent the steering commands applied to the front and rear steering actuators, respectively, while T_{brake} denotes the commanded braking torque. The actual steering angles and brake torque are generated through first-order actuator dynamics, which are described later in this chapter.

The adopted model structure provides a high-fidelity representation of vehicle dynamics while remaining suitable for implementation within the

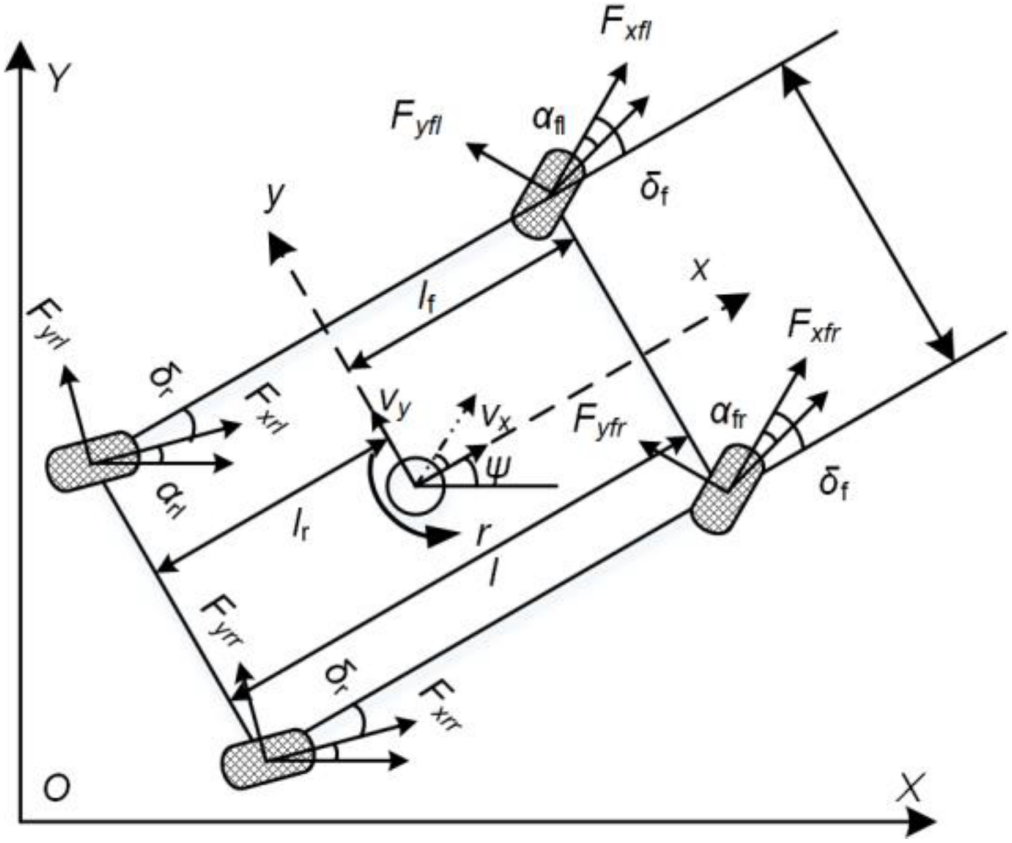


Figure 2.2: Schematic representation of the nonlinear four-wheel vehicle model including vehicle states, steering angles, and tyre force components. [9]

nonlinear predictive control framework. By explicitly accounting for wheel dynamics, tyre nonlinearities, and actuator behaviour, the model is capable of capturing the dominant phenomena that influence vehicle performance near the handling limits.

2.4 Tyre Force and Load Transfer Modeling

2.4.1 Pacejka-Based tyre Model

To accurately represent tyre-road interaction under aggressive driving conditions, a reduced Pacejka '96 tyre model was employed for the computation of longitudinal and lateral tyre forces. The model provides a nonlinear relationship between tyre forces, tyre slip, and vertical load, allowing the prediction model to capture force saturation effects that become significant near the handling limits.

The longitudinal tyre force is expressed as

$$F_{x0} = D_x \sin\left[C_x \tan^{-1}\left(B_x s - E_x\left(B_x s - \tan^{-1}(B_x s)\right)\right)\right] \tag{2.3}$$

where s denotes the longitudinal slip ratio, while B_x, C_x, D_x, and E_x are the Pacejka stiffness, shape, peak, and curvature factors, respectively.

Similarly, the lateral tyre force is computed as

$$F_{y0} = D_y \sin\left[C_y \tan^{-1}\left(B_y \alpha - E_y\left(B_y \alpha - \tan^{-1}(B_y \alpha)\right)\right)\right] + S_{vy} \tag{2.4}$$

where α is the tyre slip angle and S_{vy} represents the camber-induced lateral force contribution.

$$\alpha = -\frac{V_y}{|V_x|} \tag{2.5}$$

2.4.2 Combined Slip Effects

When a tyre simultaneously generates longitudinal and lateral forces, the available friction potential must be shared between both force components. To account for this behaviour, combined slip correction factors are introduced.

The longitudinal force reduction factor is defined as

$$G_{xa} = \cos\left(C_{xa} \tan^{-1}(B_{xa}\alpha)\right) \tag{2.6}$$

while the lateral force reduction factor is expressed as

$$G_{yk} = \cos\left(C_{yk} \tan^{-1}(B_{yk} s)\right). \tag{2.7}$$

The final tyre forces become

$$F_x = F_{x0} G_{xa} \tag{2.8}$$

and

$$F_y = F_{y0} G_{yk}. \tag{2.9}$$

2.4.3 Rolling Resistance Moment

In addition to longitudinal and lateral tyre forces, a rolling resistance moment is included to account for energy dissipation at the tyre-road interface.

The rolling resistance moment is modeled as

$$M_{rr} = -F_z R_0 \left(q_{sy1} \tan^{-1}\left(\frac{V_r}{V_0}\right) + q_{sy2} \frac{F_x}{F_{z0}} \right) \tag{2.10}$$

where R_0 is the effective wheel radius and V_r is the wheel rolling velocity.

2.4.4 Dynamic Load Transfer

The force generation capability of a tyre is strongly influenced by the vertical load acting on the contact patch. During vehicle manoeuvres, the normal loads acting on the wheels are not constant but vary as a consequence of vehicle accelerations. This phenomenon, commonly referred to as load transfer, modifies the distribution of vertical forces among the four wheels and directly affects the available tyre-road friction.[4]

Longitudinal load transfer occurs during acceleration and braking manoeuvres. Under acceleration, a portion of the vehicle load is transferred from the front axle to the rear axle, increasing the vertical loads acting on the rear tyres. Conversely, braking causes the load to shift towards the front axle, increasing the front tyre loads while reducing those at the rear axle.

Lateral load transfer arises during cornering due to the lateral acceleration of the vehicle. As the vehicle negotiates a turn, the vertical load is transferred from the inside wheels to the outside wheels. This effect becomes increasingly significant as lateral acceleration increases and can substantially alter the force generation characteristics of each tyre. [10]. These phenomena are shown in figure 2.3

To account for these effects, the adopted vehicle model computes the vertical load acting on each wheel individually. The resulting wheel loads

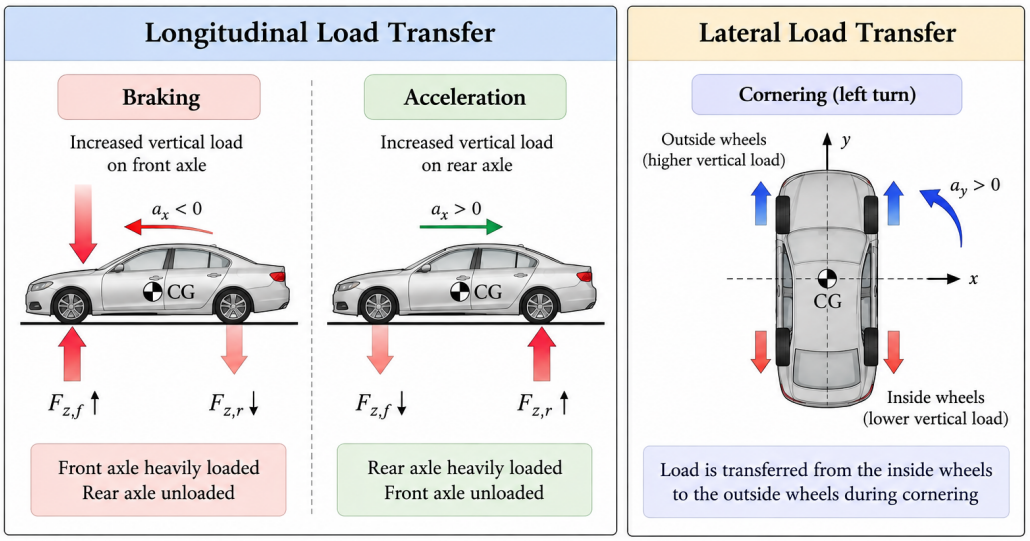


Figure 2.3: Illustration of longitudinal and lateral load transfer effects during acceleration, braking, and cornering manoeuvres.

are then used as inputs to the Pacejka tyre model, allowing the influence of load transfer on longitudinal and lateral force generation to be represented within the NMPC prediction model.

The inclusion of dynamic load transfer improves the physical fidelity of the model and enables a more realistic prediction of vehicle behaviour during aggressive manoeuvres near the limits of tyre adhesion. This is particularly important for path tracking applications involving rapid steering inputs, emergency obstacle avoidance, and high-speed cornering scenarios where significant variations in wheel loading occur.

2.5 Vehicle Equations of Motion

The motion of the vehicle is described through a set of nonlinear differential equations representing the translational, rotational, and wheel dynamics. The equations are formulated in the vehicle-fixed reference frame and are used by the NMPC controller to predict future vehicle behaviour over the prediction horizon.

2.5.1 Translational Dynamics

The translational motion of the vehicle is described by the longitudinal velocity V_x and lateral velocity V_y expressed in the body-fixed reference frame. The evolution of these states is determined by the tyre forces generated at each wheel together with the coupling effects introduced by the vehicle yaw motion.

The longitudinal dynamics are obtained by summing the longitudinal force contributions acting on the vehicle body and are expressed as

$$\dot{V}_x = \frac{1}{m}\left(F_{x,FL}\cos\delta_{FL} + F_{x,FR}\cos\delta_{FR} + F_{x,RL}\cos\delta_{RL} + F_{x,RR}\cos\delta_{RR} - C_{rr}V_x^2\right) + V_y r \tag{2.11}$$

where m is the vehicle mass, $F_{x,i}$ denotes the longitudinal force generated at wheel i, δ_i is the corresponding wheel steering angle, C_{rr} represents the resistance coefficient, and r is the yaw rate. The term $V_y r$ accounts for the coupling between longitudinal and lateral motion arising from the rotating vehicle reference frame.

Similarly, the lateral dynamics are expressed as

$$\dot{V}_y = \frac{1}{m}\Big(F_{x,FL}\sin\delta_{FL} + F_{y,FL}\cos\delta_{FL} + F_{x,FR}\sin\delta_{FR} + F_{y,FR}\cos\delta_{FR} \tag{2.12}$$

$$+F_{x,RL}\sin\delta_{RL} + F_{y,RL}\cos\delta_{RL} + F_{x,RR}\sin\delta_{RR} + F_{y,RR}\cos\delta_{RR}\Big) - V_x r$$

where m is the vehicle mass, $F_{y,i}$ denotes the lateral force generated at wheel i, δ_i is the corresponding wheel steering angle, and r is the yaw rate. The term $V_x r$ represents the inertial coupling between the longitudinal and lateral motions arising from the rotating body-fixed reference frame. Physically, it accounts for the lateral acceleration generated when the vehicle travels forward while simultaneously undergoing a yaw motion. [4]

The adopted formulation allows the influence of each tyre to be represented individually, providing a more accurate description of vehicle behaviour near the handling limits compared to simplified single-track models. This level of detail is particularly important for the prediction of highly transient manoeuvres where tyre saturation and force redistribution significantly affect vehicle response.

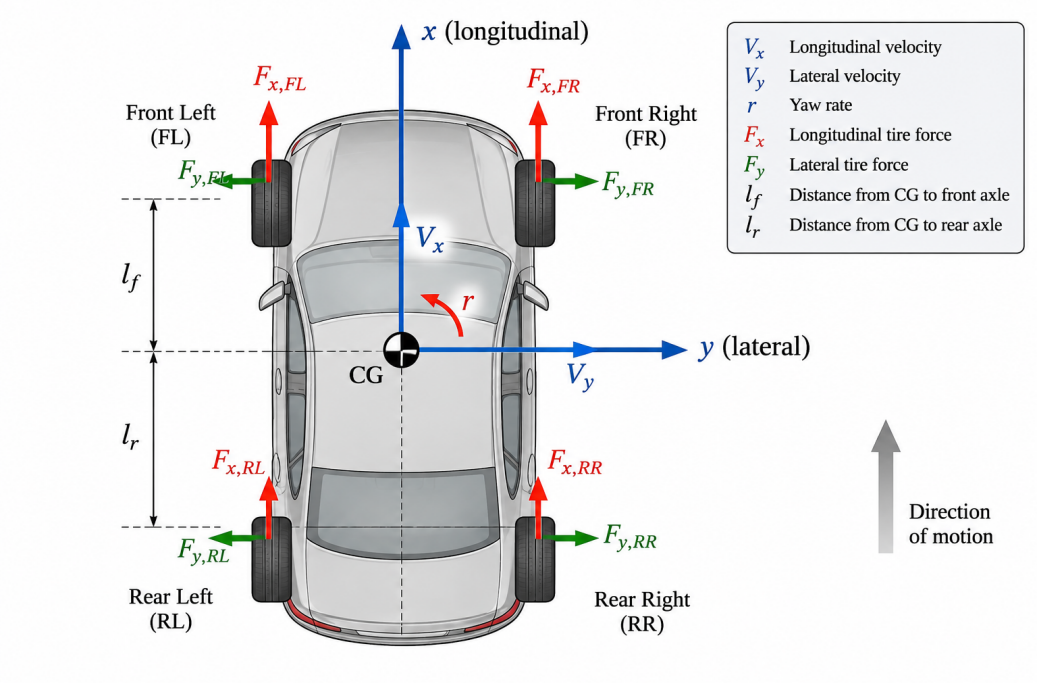


Figure 2.4: Longitudinal and lateral force components acting on the vehicle body-fixed reference frame.

2.5.2 Yaw Dynamics

The rotational motion of the vehicle about the vertical axis is described by the yaw rate r. The yaw acceleration is obtained from the rotational form of

Newton's second law,

$$I_z \dot{r} = M_z \tag{2.13}$$

where I_z denotes the yaw moment of inertia and M_z represents the total moment generated by the tyre forces about the vehicle centre of gravity.

$$\dot{r} = \frac{1}{I_z} \left(M_{FL} + M_{FR} + M_{RL} + M_{RR} \right) \tag{2.14}$$

The total yaw moment is obtained by summing the individual contributions generated by the longitudinal and lateral tyre forces acting at each wheel. Both axle distances and track-width effects are included, allowing asymmetric force generation to influence the vehicle rotational dynamics.

2.5.3 Wheel Rotational Dynamics

In addition to the vehicle translational and rotational motion, the angular velocity of each wheel is included as a state of the prediction model. The wheel rotational dynamics are required for the computation of tyre slip ratios, which directly influence the longitudinal and lateral tyre force generation.

The wheel dynamics are obtained by applying the rotational form of Newton's second law to each wheel,

$$J_w \dot{\omega} = T_{act} - F_x R + M_{rr} \tag{2.15}$$

where J_w denotes the wheel rotational inertia, ω is the wheel angular velocity, T_{act} is the applied braking torque, F_x is the longitudinal tyre force, R is the effective wheel radius, and M_{rr} represents the rolling resistance moment.

For the front wheels, the rotational dynamics are expressed as

$$\dot{\omega}_{FL} = \frac{1}{J_{w,FL}} \left(T_{brake,front} - F_{x,FL} R_{FL} + M_{rr,FL} \right) \tag{2.16}$$

$$\dot{\omega}_{FR} = \frac{1}{J_{w,FR}} \left(T_{brake,front} - F_{x,FR} R_{FR} + M_{rr,FR} \right) \tag{2.17}$$

while the rear wheel dynamics are given by

$$\dot{\omega}_{RL} = \frac{1}{J_{w,RL}} \left(T_{brake,rear} - F_{x,RL} R_{RL} + M_{rr,RL} \right) \tag{2.18}$$

$$\dot{\omega}_{RR} = \frac{1}{J_{w,RR}} \left(T_{brake,rear} - F_{x,RR} R_{RR} + M_{rr,RR} \right). \tag{2.19}$$

The inclusion of individual wheel rotational dynamics enables the prediction model to accurately capture wheel slip behaviour during braking and cornering manoeuvres. This information is subsequently used by the tyre model to compute the nonlinear tyre forces acting on the vehicle.

2.6 Steering and Brake Actuator Dynamics

To improve the realism of the prediction model, the steering and braking systems are not assumed to respond instantaneously to control commands. Instead, first-order actuator dynamics are introduced to represent the finite response time of the physical actuators.

The actuator states consist of the front steering angle $\delta_{F,act}$, rear steering angle $\delta_{R,act}$, and applied braking torque $T_{brake,act}$. The corresponding control inputs are the commanded front steering angle D_F, commanded rear steering angle D_R, and commanded braking torque T_{brake}.

The front steering actuator is modeled as

$$\dot{\delta}_{F,act} = \frac{1}{\tau_s} \left(D_F - \delta_{F,act} \right) \tag{2.20}$$

where $\tau_s = 0.18\ s$ represents the steering actuator time constant.

Similarly, the rear steering actuator dynamics are given by

$$\dot{\delta}_{R,act} = \frac{1}{\tau_s} \left(D_R - \delta_{R,act} \right) \tag{2.21}$$

The brake actuator dynamics are described by

$$\dot{T}_{brake,act} = \frac{1}{\tau_b} \left(T_{brake} - T_{brake,act} \right) \tag{2.22}$$

where $\tau_b = 0.05\ s$ denotes the brake actuator time constant.

The inclusion of actuator dynamics prevents unrealistically fast control actions and allows the prediction model to better represent the behaviour of practical steering and braking systems. This is particularly important in NMPC applications, where actuator limitations can significantly influence the achievable vehicle response during aggressive manoeuvres.

Chapter Summary

This chapter presented the nonlinear prediction model adopted for the NMPC framework. A four-wheel vehicle model was introduced to capture the longitudinal, lateral, and yaw dynamics of the vehicle while accounting for indi-

vidual tyre force contributions. A reduced Pacejka-based tyre model was employed to represent the nonlinear tyre-road interaction, including combined-slip effects and dynamic load transfer. Furthermore, wheel rotational dynamics and first-order steering and brake actuator dynamics were incorporated to improve the physical realism of the model.

The resulting formulation provides a comprehensive representation of vehicle behaviour over a wide operating range and forms the internal prediction model used by the NMPC controller. Based on this model, the optimal control problem can be formulated to generate control actions that satisfy vehicle constraints while achieving the desired trajectory tracking and obstacle avoidance objectives which will be discussed in the next chapter.

Chapter 3

Optimal Control Problem Formulation and Assumptions

3.1 Introduction

The nonlinear vehicle model presented in Chapter 2 serves as the prediction model within the Nonlinear Model Predictive Control (NMPC) framework. At each sampling instant, the controller predicts the future evolution of the vehicle states over a finite prediction horizon and computes the sequence of control actions that minimizes a predefined objective function while satisfying the system constraints.

Unlike conventional feedback controllers, NMPC explicitly incorporates the nonlinear vehicle dynamics, actuator limitations, and operational constraints into the control design. This allows the controller to anticipate future vehicle behaviour and generate control actions that achieve the desired objectives while maintaining safe and physically feasible operation.

The NMPC strategy adopted in this work is formulated as a constrained optimal control problem (OCP). The optimization problem is solved repeatedly in a receding horizon manner, where only the first control action of the optimal sequence is applied to the vehicle before the optimization is repeated using updated state measurements. [6]

This chapter presents the mathematical formulation of the optimal control problem, including the cost function design, system constraints, prediction horizon selection, and solver configuration. Particular attention is given to the implementation developed using CasADi and ACADOS, which enables real-time solution of the nonlinear optimization problem.

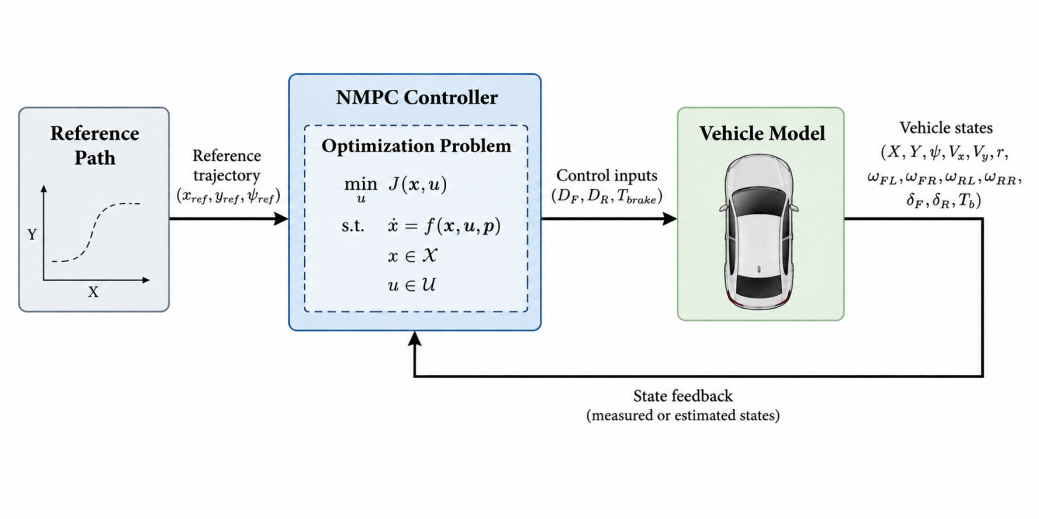


Figure 3.1: Receding horizon implementation of the NMPC framework adopted in this work.

.

3.2 NMPC Problem Formulation

The objective of the NMPC controller is to determine the optimal sequence of steering and braking commands that minimizes a predefined cost function while satisfying the vehicle dynamics and operational constraints. To achieve this, the vehicle model introduced in Chapter 2 is embedded within a finite-horizon optimal control problem (OCP).[6]

The nonlinear vehicle dynamics can be represented in compact form as

$$\dot{x}(t) = f(x(t), u(t), p(t)) \tag{3.1}$$

where $x \in \mathbb{R}^{n_x}$ is the state vector, $u \in \mathbb{R}^{n_u}$ is the control input vector, and p denotes the time-varying parameters used by the prediction model. The nonlinear function $f(\cdot)$ represents the vehicle dynamics described in Chapter 2.

At each sampling instant, the controller predicts the future evolution of the system over a finite prediction horizon of length T and computes the optimal control sequence

$$U = \{u_0, u_1, \ldots, u_{N-1}\} \tag{3.2}$$

that minimizes a performance index while satisfying the system dynamics and constraints.

The resulting optimal control problem can be written as

$$
\begin{aligned}
\min_{x_k, u_k} \quad & \sum_{k=0}^{N-1} L(x_k, u_k) + L_f(x_N) \\
\text{s.t.} \quad & x_{k+1} = f_d(x_k, u_k) \\
& x_k \in \mathcal{X} \\
& u_k \in \mathcal{U} \\
& h(x_k, u_k) \leq 0 \\
& x_0 = x_{\text{meas}}
\end{aligned}
\tag{3.3}
$$

where $L(\cdot)$ denotes the stage cost, $L_f(\cdot)$ is the terminal cost, $\mathcal{X}$ and $\mathcal{U}$ represent the admissible state and input sets, and $h(\cdot)$ collects the nonlinear constraints imposed on the system.

The optimization problem is solved repeatedly in a receding horizon manner. After each optimization step, only the first control input of the optimal sequence is applied to the vehicle, while the remaining inputs are discarded. At the next sampling instant, the prediction horizon is shifted forward and the optimization problem is solved again using the updated vehicle state.

3.3 Cost Function Design

The objective of the NMPC controller is to minimize the deviation from the desired trajectory while simultaneously limiting excessive control actions. To achieve this, a nonlinear least-squares (NONLINEAR_LS) cost formulation is adopted within the ACADOS framework.

The stage cost is defined as

$$
J = \sum_{k=0}^{N-1} \|y_k - y_{ref,k}\|_W^2 + \|y_N - y_{ref,N}\|_{W_e}^2 \tag{3.4}
$$

where W and W_e are positive-definite weighting matrices and y_k represents the vector of cost variables evaluated at prediction step k.

The stage cost vector adopted in this work is defined as

$$y = \begin{bmatrix} e_{hea} \\ e_{crt} \\ \dfrac{D_F}{0.1} \\ \dfrac{D_R}{0.1} \\ \dfrac{T_{brake}}{1000} \\ \dfrac{v_{ref} - V_x}{10} \end{bmatrix} \tag{3.5}$$

where e_{hea} denotes the heading error, e_{crt} represents the cross-track error, D_F and D_R are the commanded front and rear steering angles, T_{brake} is the braking torque command, and $v_{ref} - V_x$ is the vehicle speed tracking error. The numbers in denominator of the cost variables are present to make every term into the same magnitude.

The terminal cost vector is defined as

$$y_e = \begin{bmatrix} e_{hea} \\ e_{crt} \\ \dfrac{v_{ref} - V_x}{10} \end{bmatrix} \tag{3.6}$$

The weighting matrices used in the optimization problem are

$$W = \mathrm{diag}\,(1,\, 25,\, 1,\, 10,\, 1,\, 35) \tag{3.7}$$

and

$$W_e = \mathrm{diag}\,(1,\, 25,\, 35)\,. \tag{3.8}$$

A larger weight is assigned to the speed tracking error and cross-track error, reflecting their importance in maintaining both vehicle stability and path-following performance. The steering and braking commands are also penalized to avoid excessive actuator activity and to promote smoother control actions. Furthermore, a higher penalty is applied to rear steering inputs to limit aggressive rear-wheel steering behaviour during obstacle avoidance manoeuvres.

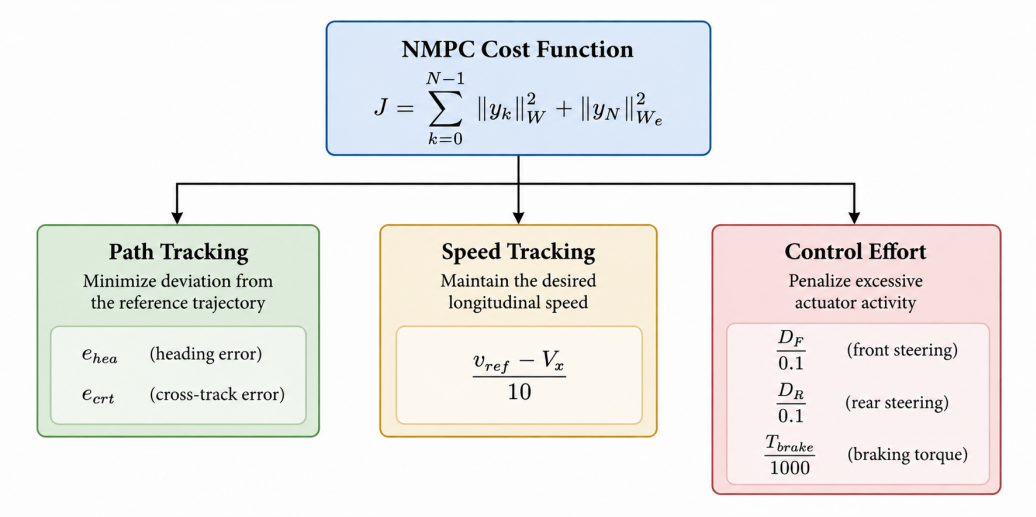


Figure 3.2: Components of the NMPC cost function used in the optimization problem.

3.4 Constraints

To ensure physically feasible and safe vehicle behaviour, the NMPC optimization problem incorporates state, input, and tyre-related constraints. These constraints restrict the solution space of the optimizer and prevent the controller from generating commands that exceed vehicle limitations.

The constraints are enforced at every prediction step throughout the horizon and are incorporated directly into the optimal control problem solved by ACADOS.

3.4.1 State Constraints

The vehicle states are bounded to maintain physically meaningful operating conditions and to improve numerical robustness of the optimization process. The state constraints can be expressed as

$$x_{\min} \leq x_k \leq x_{\max} \tag{3.9}$$

where the lower and upper bounds are defined according to the admissible operating range of the vehicle model.

Table 3.1: State constraints used in the NMPC formulation.

State	Lower Bound	Upper Bound
V_x [m/s]	5	80
V_y [m/s]	-10	10
r [rad/s]	-70	70
ω_{FL} [rad/s]	2.5	450
ω_{FR} [rad/s]	2.5	450
ω_{RL} [rad/s]	2.5	450
ω_{RR} [rad/s]	2.5	450
$T_{brake,act}$ [Nm]	-1000	1000

3.4.2 Input Constraints

The steering and braking commands generated by the controller are constrained according to the actuator capabilities. The input constraints are defined as

$$u_{\min} \leq u_k \leq u_{\max} \tag{3.10}$$

The control inputs generated by the NMPC controller are constrained according to the physical limitations of the steering and braking actuators.

Table 3.2: Input constraints used in the NMPC formulation.

Input	Lower Bound	Upper Bound
D_F [rad]	-1.35	1.35
D_R [rad]	-1.10	1.10
T_{brake} [Nm]	-1000	1000

where the lower and upper bounds for each control input are reported in Table 3.2.

3.4.3 Soft Constraints and Slack Variables

In addition to the hard state and input constraints, soft constraints are introduced to limit the longitudinal slip ratio of each wheel. These constraints improve vehicle stability while avoiding optimization infeasibility in highly demanding manoeuvres.

The longitudinal slip constraints are formulated as

$$-0.25 \leq s_i \leq 0.25 \qquad i \in \{FL, FR, RL, RR\} \tag{3.11}$$

where s_i denotes the longitudinal slip ratio of the corresponding wheel. To allow temporary and controlled constraint violations when necessary, slack variables are incorporated into the optimization problem. Constraint violations are penalized through additional cost terms, ensuring that the optimizer only exceeds the prescribed limits when required to maintain feasibility. The slack-variable penalties are incorporated through quadratic and linear

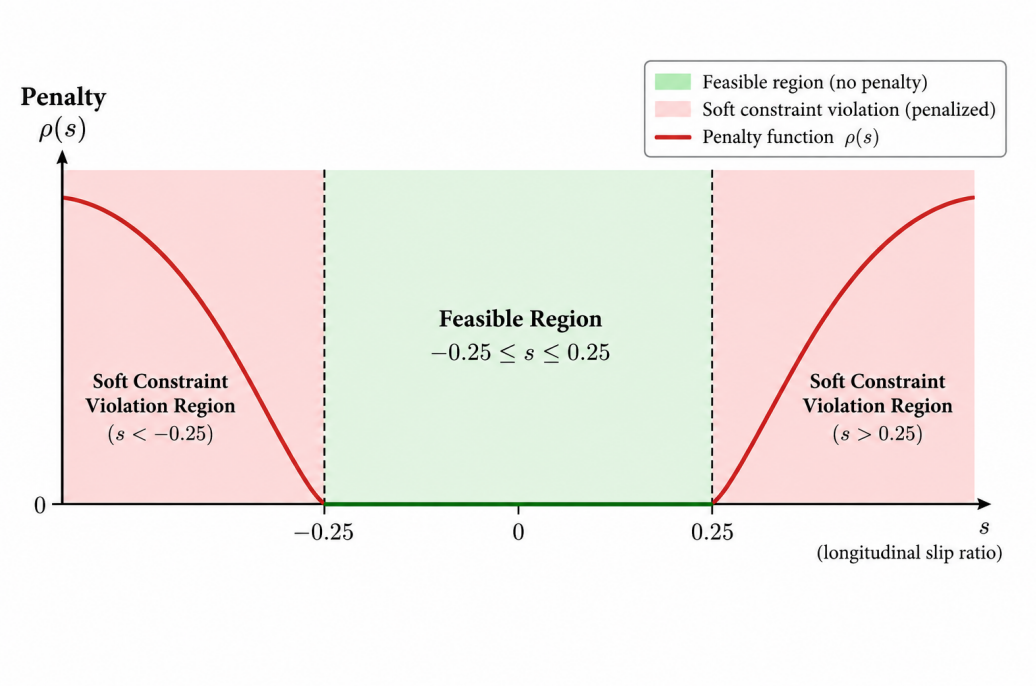


Figure 3.3: Soft longitudinal slip constraints imposed on each wheel within the NMPC formulation.

penalty terms within the cost function, discouraging unnecessary constraint violations while preserving numerical robustness of the optimization process.

3.5 Prediction Horizon and Discretization

The prediction horizon defines the future time interval over which the NMPC controller predicts the vehicle behaviour and computes the optimal control actions. The selection of the horizon length and discretization strategy significantly influences both control performance and computational efficiency.

In this work, the prediction horizon is discretized into

$$N = 20 \tag{3.12}$$

shooting intervals over a total horizon duration of

$$T = 1.5 \text{ s}. \tag{3.13}$$

As a result, the prediction horizon consists of 21 discretization nodes, at which the future vehicle states are predicted, while the control inputs are optimized over the 20 intervals connecting these nodes.

Unlike conventional implementations that employ uniform discretization, a non-uniform time distribution is adopted in order to increase prediction accuracy in the near future, where control actions have the greatest influence on vehicle behaviour. The normalized node locations are computed as

$$\tau_i = \left(\frac{i}{N}\right)^{\alpha}, \qquad i = 0, \ldots, N \tag{3.14}$$

where α is a density distribution factor controlling the spacing of the prediction nodes.

The corresponding time intervals are then obtained as

$$\Delta t_i = T\left(\tau_{i+1} - \tau_i\right), \qquad i = 0, \ldots, N-1 \tag{3.15}$$

with

$$\alpha = 1.5. \tag{3.16}$$

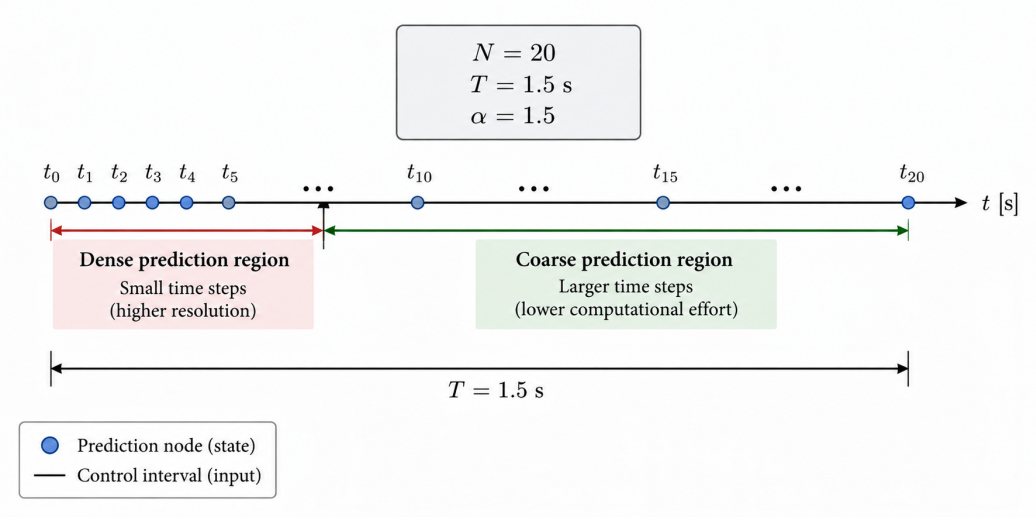


Figure 3.4: Non-uniform prediction horizon discretization adopted in the NMPC formulation.

Since $\alpha > 1$, the resulting discretization produces smaller time steps near the beginning of the prediction horizon and progressively larger time steps towards its end as shown in figure 3.4. Consequently, the controller achieves a finer resolution for short-term predictions while maintaining a sufficiently long prediction horizon without introducing an excessive computational burden.

This discretization strategy is particularly advantageous in emergency obstacle avoidance scenarios, where accurate short-term predictions are essential for generating timely steering and braking actions. At the same time, the larger intervals at the end of the horizon preserve the controller's ability to anticipate future vehicle behaviour while reducing the overall complexity of the optimization problem.

3.6 ACADOS Solver Configuration

The optimal control problem formulated in the previous sections is solved using the ACADOS optimization framework. ACADOS is specifically designed for embedded and real-time nonlinear optimal control applications, providing efficient numerical algorithms for solving constrained nonlinear model predictive control problems.

The implementation developed in this work employs a Sequential Quadratic Programming (SQP) scheme in combination with a multiple-shooting discretization of the nonlinear vehicle model. At each sampling instant, the nonlinear optimal control problem is approximated by a sequence of quadratic programming (QP) subproblems, which are solved iteratively until convergence.[6]

The solver configuration was selected to achieve a suitable balance between numerical robustness, solution accuracy, and computational efficiency during highly dynamic emergency manoeuvres.

3.6.1 Nonlinear Programming Solver

The nonlinear optimal control problem is solved using the Sequential Quadratic Programming (SQP) algorithm available within ACADOS. SQP is a widely adopted method for nonlinear constrained optimization, where the original nonlinear problem is approximated through a sequence of quadratic programming subproblems.

At each SQP iteration, the nonlinear dynamics and constraints are linearized around the current solution estimate, while the objective function is approximated by a quadratic model. The resulting QP subproblem is

solved to obtain an improved solution, and the procedure is repeated until convergence criteria are satisfied.

3.6.2 Quadratic Programming Solver

Each QP subproblem generated by the SQP algorithm is solved using the HPIPM (High-Performance Interior Point Method) solver with partial condensing.

Partial condensing reduces the dimensionality of the QP problem while preserving the essential structure of the optimal control formulation. In the present implementation, a condensing horizon of

$$N_c = 5 \tag{3.17}$$

is adopted, providing an effective compromise between computational speed and numerical efficiency.

3.6.3 Numerical Integration Method

The vehicle dynamics are discretized using the Implicit Runge–Kutta (IRK) integration scheme available within ACADOS. Compared with explicit integration methods, IRK provides improved numerical stability when simulating highly nonlinear vehicle dynamics.

For each prediction interval, the integration procedure is performed using 25 internal integration steps, allowing accurate propagation of the vehicle states throughout the prediction horizon.

3.6.4 Globalization Strategy

To improve convergence robustness, the optimization process employs the Merit Backtracking globalization strategy. This approach combines the objective function and constraint violations into a merit function used to evaluate individual optimization steps.

If a proposed SQP step does not provide sufficient improvement of the merit function, the step size is progressively reduced until an acceptable descent condition is achieved. This mechanism improves convergence reliability, particularly during aggressive obstacle avoidance manoeuvres where highly nonlinear vehicle behaviour may be encountered.

3.6.5 Warm Starting

Warm starting is enabled for the QP solver to accelerate convergence between successive NMPC iterations. Since consecutive optimization problems are solved at closely spaced sampling instants, the solution obtained during the previous control cycle provides a suitable initial guess for the subsequent optimization problem.

This strategy reduces the number of iterations required for convergence and improves real-time computational performance.

3.6.6 Regularization Strategy

To improve numerical robustness, the CONVEXIFY regularization method is employed within ACADOS. This technique modifies the Hessian approximation when necessary to ensure that the resulting QP subproblem remains numerically well conditioned.

In addition, a Levenberg–Marquardt regularization parameter of

$$\lambda = 10^{-2} \tag{3.18}$$

is introduced to improve stability during the solution of highly nonlinear optimization problems.

3.6.7 Solver Tolerances

The convergence criteria adopted for the SQP solver are summarized in Table 3.3. These tolerances define the acceptable levels of optimality, equality constraint satisfaction, inequality constraint satisfaction, and complementarity residuals.

A maximum of 3000 SQP iterations is permitted to ensure convergence under demanding operating conditions. [11] The selected ACADOS con-

Table 3.3: ACADOS solver tolerances.

Parameter	Value
Maximum SQP iterations	3000
Optimality tolerance	10^{-2}
Equality constraint tolerance	10^{-2}
Inequality constraint tolerance	10^{-2}
Complementarity tolerance	10^{-2}

figuration combines a Sequential Quadratic Programming framework with

efficient QP solution techniques and robust numerical integration methods. This setup enables the real-time solution of the nonlinear optimal control problem while maintaining numerical stability during highly dynamic obstacle avoidance manoeuvres. The resulting controller is subsequently evaluated through simulation studies presented in Chapter 4.

Chapter Summary

This chapter presented the formulation of the Nonlinear Model Predictive Control (NMPC) framework adopted for autonomous obstacle avoidance. The nonlinear vehicle model developed in Chapter 2 was incorporated into a finite-horizon optimal control problem, where steering and braking actions are computed by minimizing a nonlinear least-squares cost function while satisfying state, input, and tyre-slip constraints.

The cost function was designed to balance trajectory tracking performance, speed regulation, and control effort, whereas soft constraints were introduced to preserve feasibility during highly dynamic manoeuvres. Furthermore, a non-uniform prediction horizon discretization was employed to improve short-term prediction accuracy while maintaining computational efficiency.

Finally, the ACADOS solver configuration was presented, including the SQP optimization scheme, HPIPM quadratic programming solver, IRK integration method, warm-start strategy, and regularization techniques used to achieve real-time optimization performance. The resulting NMPC controller is evaluated in the simulation studies presented in the next chapter.

Chapter 4

Simulation Environment and Results

4.1 Introduction

This chapter presents the simulation studies conducted to evaluate the performance of the proposed Nonlinear Model Predictive Control (NMPC) framework for autonomous obstacle avoidance. The controller developed in the previous chapters is implemented within a MATLAB/Simulink environment and tested under an emergency steering manoeuvre representation

The performance of the NMPC controller is investigated at three different initial vehicle speeds of 60 km/h, 65 km/h, and 70 km/h. These operating conditions are selected to assess the capability of the controller to maintain accurate path tracking and vehicle stability as the severity of the manoeuvre increases.

The simulation results are analysed using trajectory tracking performance, vehicle dynamic response, and control effort metrics. Particular attention is given to cross-track error, heading error, vehicle velocities, yaw rate behaviour, tyre slip characteristics, and the steering and braking actions generated by the controller throughout the manoeuvre.

4.2 Emergency Evasive Manoeuvre

To evaluate the performance of the proposed NMPC controller, a demanding evasive steering manoeuvre was designed and implemented within the simulation environment. The manoeuvre was selected to generate significant lateral and yaw dynamics while requiring accurate path tracking and stable vehicle behaviour.

Unlike conventional trajectory-tracking tests performed under mild operating conditions, the selected manoeuvre imposes rapid directional changes that challenge both the prediction capabilities of the controller and the dynamic limits of the vehicle. Consequently, it provides a suitable benchmark for assessing the effectiveness of the proposed NMPC framework under highly transient driving conditions.

The reference trajectory consists of three consecutive path segments: an entry straight section, a constant-radius turn, and an exit straight section. This geometry enables the vehicle to transition from steady-state motion into a highly dynamic cornering phase before returning to straight-line driving.

4.2.1 Reference Path Design

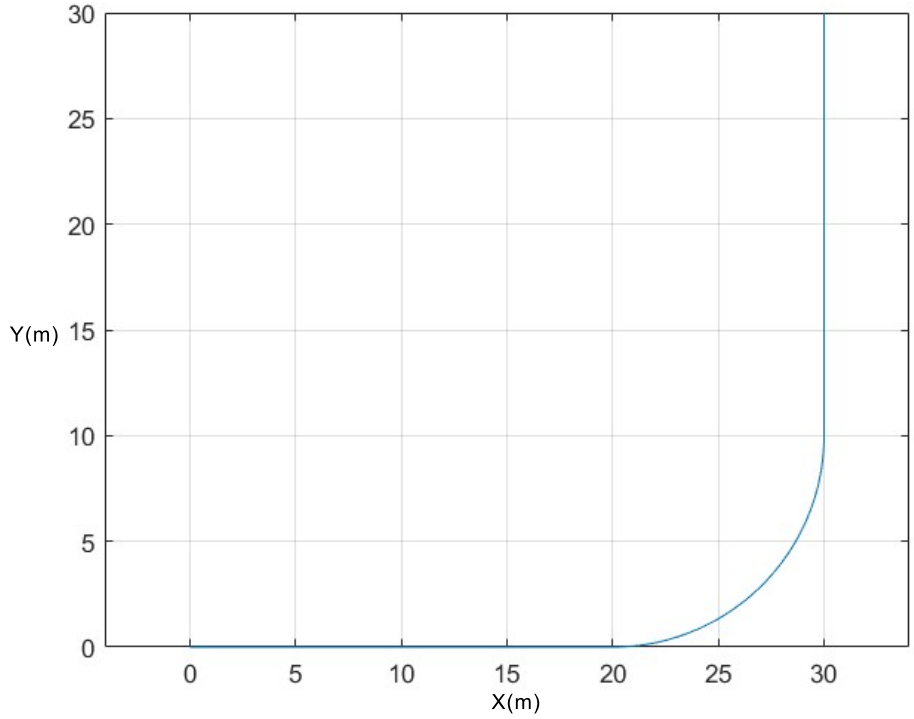


Figure 4.1: Reference evasive manoeuvre trajectory used for controller evaluation.

The reference trajectory adopted in this work is illustrated in Figure 4.1. The manoeuvre begins with a 20 m straight section that allows the vehicle to stabilize before entering the turning region. This is followed by a 90°

constant-radius turn with a radius of 10 m, after which the vehicle exits onto a second 20 m straight section.

The trajectory was generated using the path definition

$$\text{Path Design} = \begin{bmatrix} 20 & 0 \\ 10\pi/2 & 1/10 \\ 20 & 0 \end{bmatrix} \tag{4.1}$$

where the first column represents the segment length and the second column specifies the path curvature. A curvature value of zero corresponds to straight-line motion, while a curvature of 0.1 m generates the constant-radius turning segment.

The resulting path has a total length of approximately

$$L = 20 + \frac{\pi}{2}(10) + 20 = 55.71 \text{ m}. \tag{4.2}$$

This trajectory was selected because it produces significant lateral acceleration demands and therefore provides a representative test of the vehicle's handling performance and the controller's ability to maintain accurate path tracking.

4.2.2 Vehicle Initial Conditions

At the beginning of each simulation, the vehicle is positioned at the start of the reference trajectory with zero cross-track error and zero heading error. The initial lateral velocity and yaw rate are set to zero, corresponding to steady straight-line motion prior to the manoeuvre.

The wheel rotational speeds are initialized consistently with the selected vehicle speed to ensure physically realistic operating conditions. Furthermore, the front steering angle, rear steering angle, and braking actuator states are initialized to zero.

4.2.3 Tested Vehicle Speeds

The proposed NMPC controller was evaluated at three different initial vehicle speeds:

$$V_{x,0} = \{60,\ 65,\ 70\} \text{ km/h}. \tag{4.3}$$

These test cases were selected to progressively increase the severity of the manoeuvre and to investigate the controller's capability to maintain path-tracking accuracy and vehicle stability as the operating conditions become more demanding.

For all simulations, the vehicle model, controller configuration, prediction horizon, optimization settings, and reference trajectory were kept unchanged. Consequently, the influence of vehicle speed on the closed-loop system performance can be evaluated in a consistent and systematic manner.

4.3 Path Tracking Performance

The primary objective of the proposed NMPC controller is to accurately track the reference trajectory while maintaining stable vehicle behaviour throughout the manoeuvre. To evaluate the path-following capability of the controller, the vehicle response was analysed at initial speeds of 60 km/h, 65 km/h, and 70 km/h.

The tracking performance is assessed using the vehicle trajectory, cross-track error, and heading error. These metrics provide insight into the ability of the controller to follow the desired path under increasingly demanding operating conditions.

4.3.1 Vehicle Trajectory Tracking

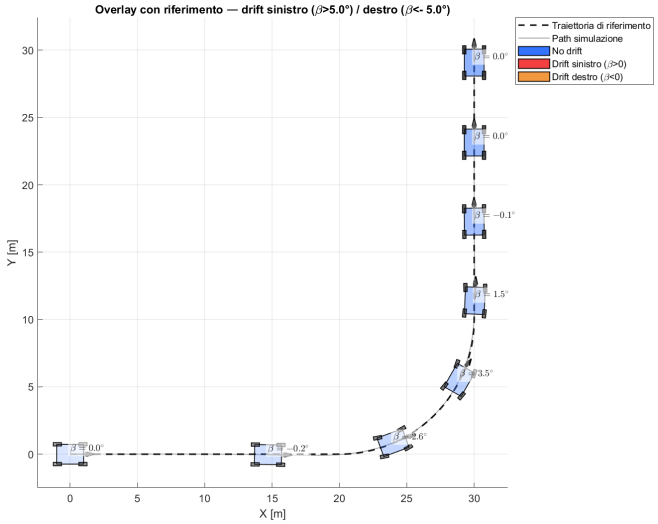
Figure 4.2 compares the reference trajectory with the trajectories generated by the NMPC controller for the three tested vehicle speeds.

Visual inspection of the results allows the evaluation of the controller's ability to accurately negotiate the turning section of the manoeuvre while maintaining stable path-following behaviour. Particular attention is given to the entry and exit regions of the curve, where rapid changes in vehicle heading are required. An additional indicator of vehicle stability is the sideslip angle, which remained below the predefined drift threshold of 5° for all investigated cases. For the 60 km/h scenario, the maximum recorded sideslip angle was approximately 3.5°, for 65km/hr it is 3.3°, and for 70km/hr it is 2.8° indicating that the vehicle remained within a stable handling regime throughout the manoeuvre. Similar behaviour was observed for the higher-speed cases.

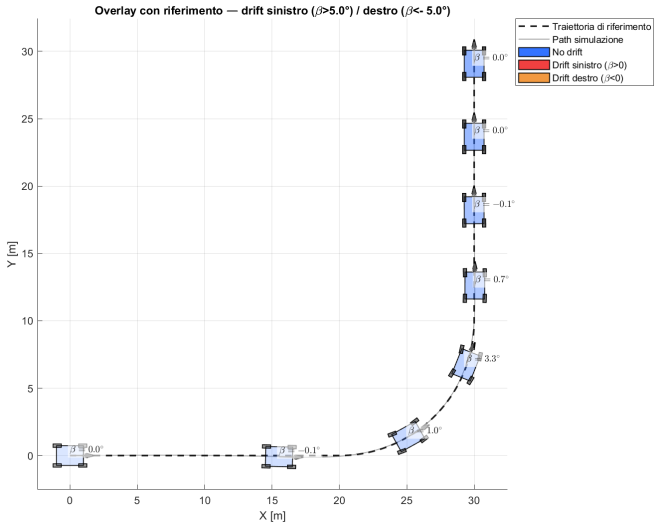
The results demonstrate that the proposed NMPC controller is capable of accurately tracking aggressive reference trajectories while simultaneously maintaining stable vehicle dynamics.

4.3.2 Cross-Track and Heading Error Analysis

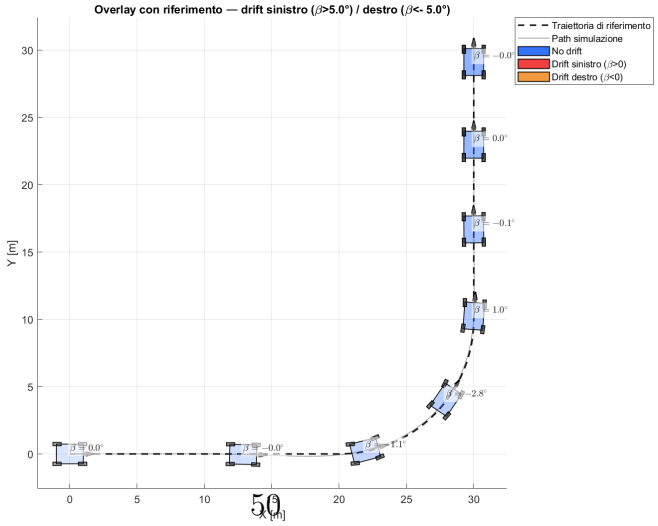
To quantitatively evaluate the path-tracking performance of the proposed NMPC controller, the evolution of the cross-track error and heading error was analysed throughout the manoeuvre. These two metrics provide direct



(a) 60 km/h

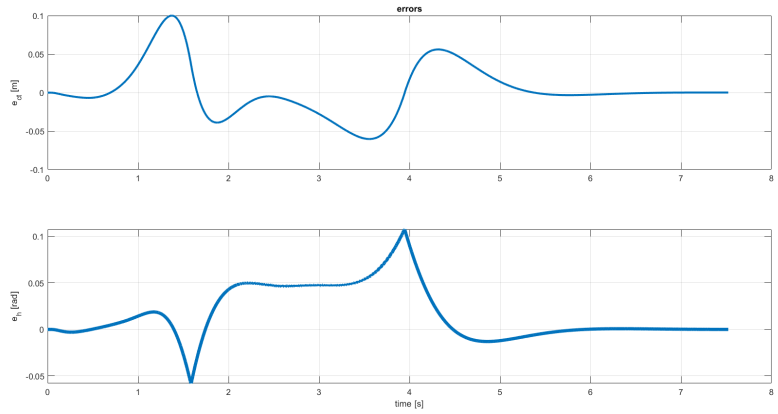


(b) 65 km/h

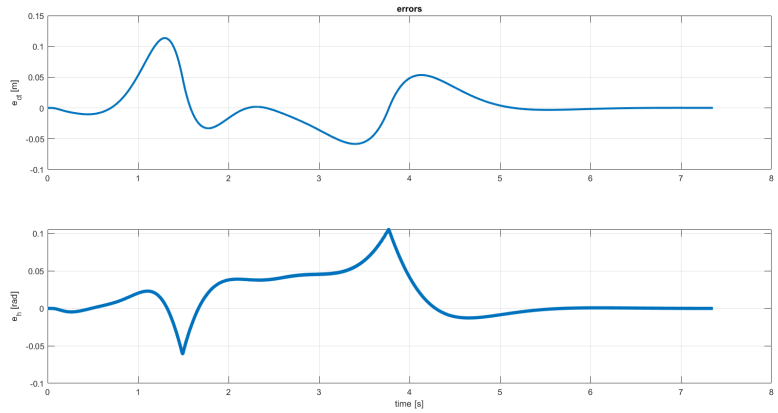


(c) 70 km/h

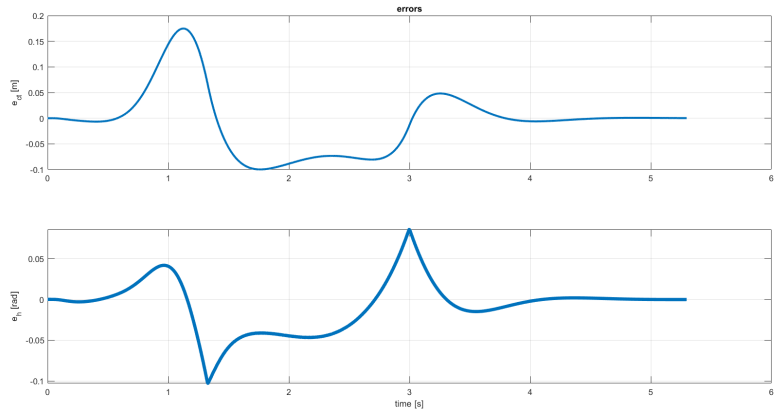
Figure 4.2: Vehicle trajectory tracking performance during the evasive manoeuvre at different initial vehicle speeds.



(a) 60 km/h



(b) 65 km/h



(c) 70 km/h

Figure 4.3: Vehicle trajectory tracking performance during the evasive manoeuvre at different initial vehicle speeds.

information regarding the vehicle's ability to remain on the desired trajectory and maintain the correct orientation relative to the reference path.

Figure 4.3 presents the cross-track error e_{ct} and heading error e_h obtained during the 60 km/h simulation. Similar trends were observed for the 65 km/h and 70 km/h test cases.

The cross-track error remained small throughout the manoeuvre, with a maximum positive deviation of approximately 0.095 m and a minimum value of approximately -0.06 m for 60km/hr, and it increased to 0.11 m & -0.06 m for 65km/hr, and finally an increased value of 0.16 m & -0.1 m for the 70km/hr manoeuvre. The largest deviations occurred during the entry and exit phases of the curved section, where the vehicle was subjected to the highest lateral acceleration demands. Despite these transient deviations, the controller rapidly corrected the trajectory and returned the error to values close to zero.

The heading error exhibited a maximum value of approximately 0.10 rad (5.7°) during the most demanding portion of the turn. Following the completion of the cornering manoeuvre, the heading error rapidly converged towards zero, indicating successful stabilization of the vehicle orientation.

The relatively small magnitude of both tracking errors demonstrates the effectiveness of the NMPC controller in maintaining accurate trajectory tracking while respecting the dynamic limitations of the vehicle. Furthermore, the smooth evolution of the error signals confirms the absence of oscillatory behaviour or aggressive corrective actions, indicating stable closed-loop performance.

4.4 Vehicle Dynamic Response

In addition to accurate path tracking, the dynamic behaviour of the vehicle must be analysed to assess the effectiveness of the proposed NMPC controller. During aggressive manoeuvres, the controller must maintain vehicle stability while generating appropriate steering and braking actions to satisfy the path-following objective.

To evaluate the dynamic response, the evolution of the vehicle speed, lateral acceleration, and sideslip angle is examined. These variables provide insight into the handling characteristics of the vehicle and the controller's ability to operate near the limits of lateral dynamics without inducing instability.

4.4.1 Velocity, Lateral Acceleration and Sideslip Angle Response

Figure 4.4,Figure 4.5 and Figure 4.6 presents the evolution of vehicle speed, lateral acceleration and sideslip angle during the emergency steering manoeuvre for initial vehicle speeds of 60 km/h, 65 km/h and 70 km/h.

The longitudinal velocity decreases throughout the manoeuvre as the NMPC controller applies braking torque while simultaneously steering the vehicle along the reference path. The vehicle initially enters the manoeuvre at the prescribed speed and gradually decelerates as kinetic energy is dissipated through the braking system. The deceleration profile remains smooth for all three test cases, demonstrating coordinated longitudinal and lateral control actions.

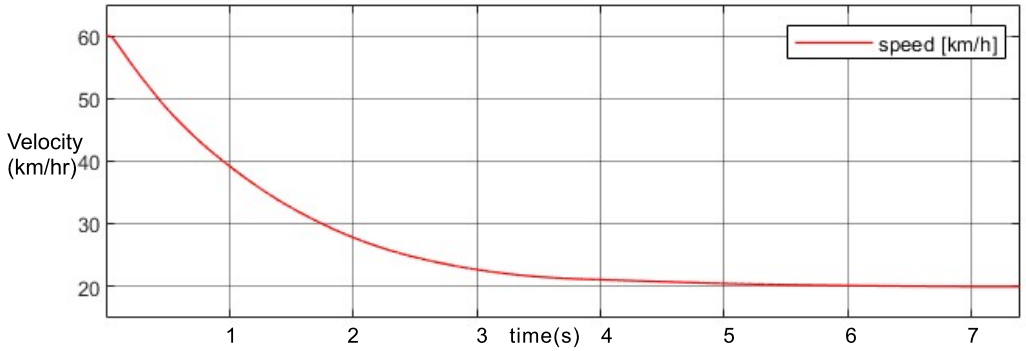
The sideslip angle response provides additional insight into vehicle stability. At 60 km/h the maximum sideslip angle remains below approximately 3.5°, indicating operation within the linear tyre region. Similar values are observed for the 65 km/h case. At 70 km/h the sideslip response exhibits larger transient excursions, reflecting the increased utilization of tyre forces during aggressive cornering and braking. Nevertheless, the sideslip angle remains well below the drift threshold of $\pm 5°$ adopted in this work, confirming that the vehicle remains in a stable handling regime.

The lateral acceleration response increases rapidly during the curved section of the path, reaching peak values corresponding to the maximum curvature demand. At 60 km/h the peak lateral acceleration remains below approximately 0.6 g, while higher initial speeds produce larger lateral loads. For the 70 km/h scenario, the peak lateral acceleration approaches 0.9 g, indicating that the vehicle is operating close to the available tyre friction limits. Despite the increased demand, the controller maintains stable vehicle behaviour throughout the manoeuvre.

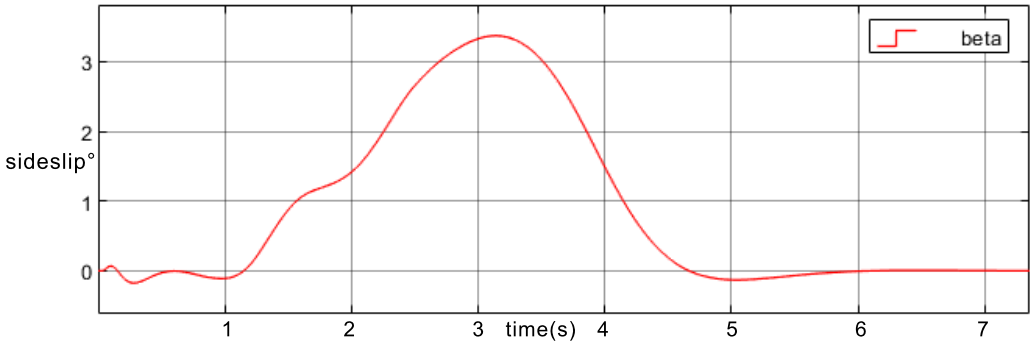
The combined velocity, lateral acceleration and sideslip responses demonstrate that the NMPC controller successfully coordinates steering and braking actions while maintaining vehicle stability across the investigated operating speeds. Although vehicle dynamic demand increases with speed, the controller preserves stable path-following performance without inducing excessive sideslip or loss of control.

4.4.2 Steering and Braking Actions

The steering and braking commands generated by the NMPC controller provide valuable insight into the control strategy adopted during the evasive manoeuvre. Figure 4.7,Figure 4.8 and Figure 4.9 present the front steer-



(a) Velocity-60 km/h

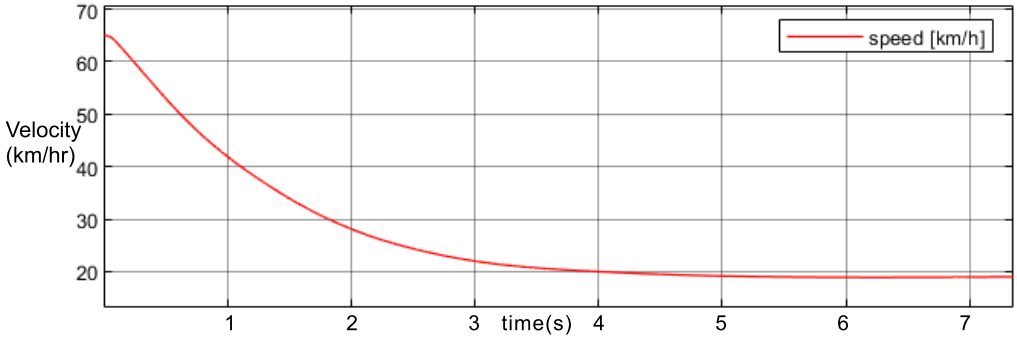


(b) Side slip-60 km/h

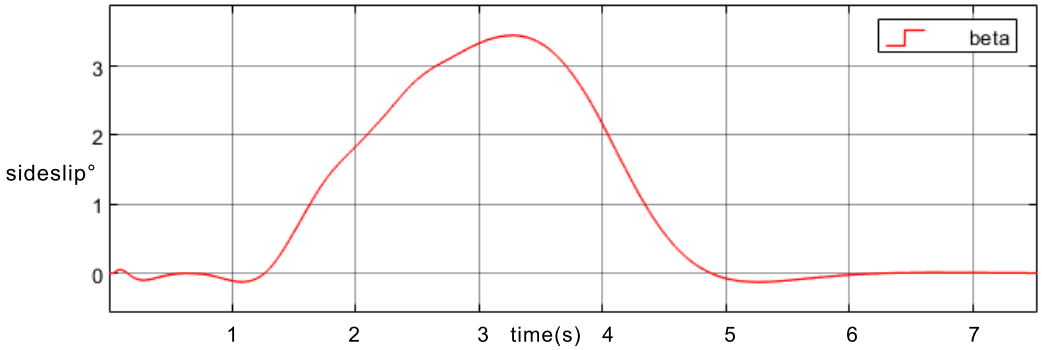


(c) Lateral acceleration-60 km/h

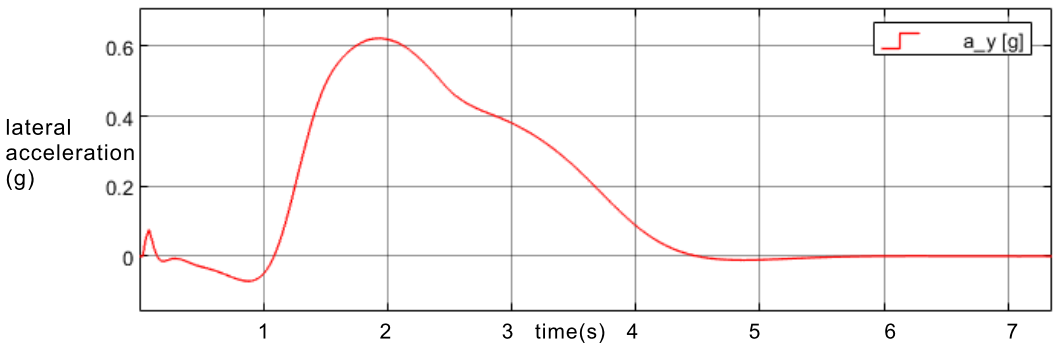
Figure 4.4: Vehicle speed, lateral acceleration and sideslip angle responses during the emergency steering manoeuvre for initial vehicle speeds 60km/hr.



(a) Velocity-65 km/h

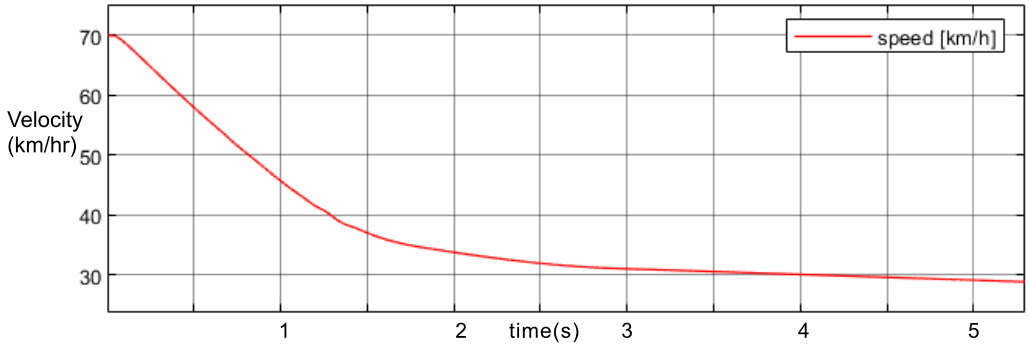


(b) Side slip-65 km/h

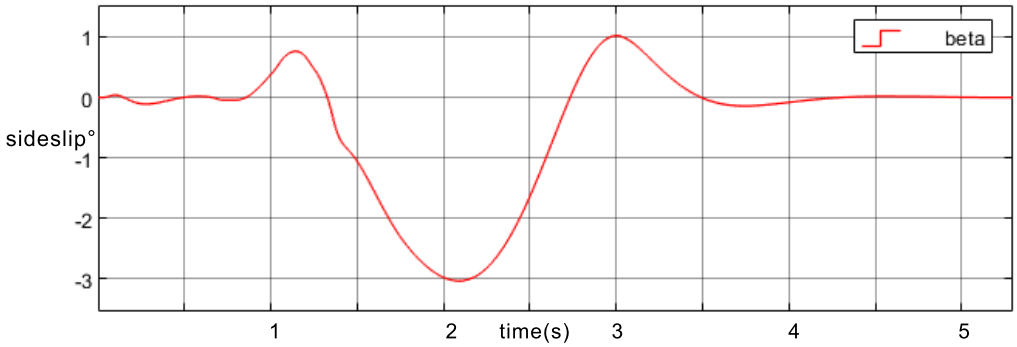


(c) Lateral acceleration-65 km/h

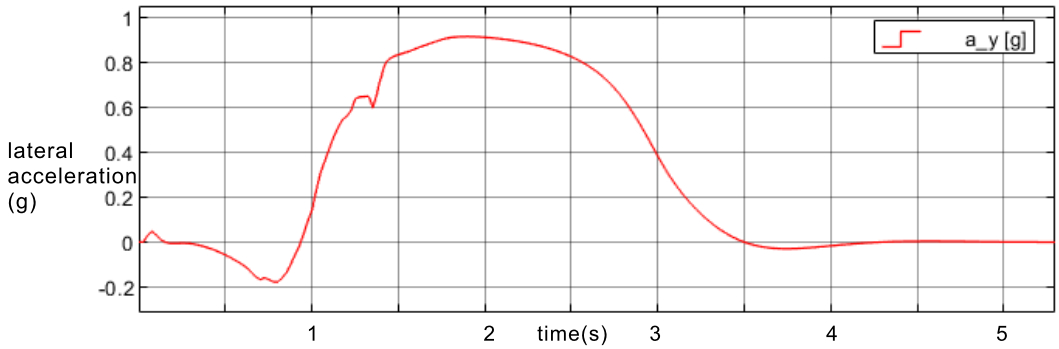
Figure 4.5: Vehicle speed, lateral acceleration and sideslip angle responses during the emergency steering manoeuvre for initial vehicle speeds 65km/hr.



(a) Velocity-70 km/h

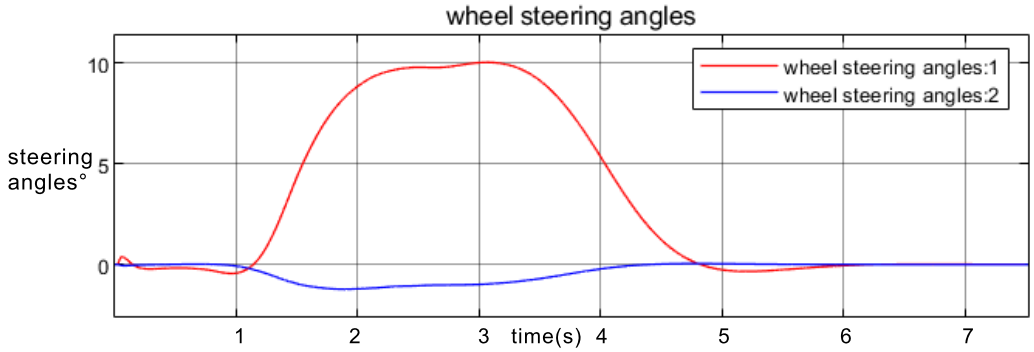


(b) Side slip-70 km/h

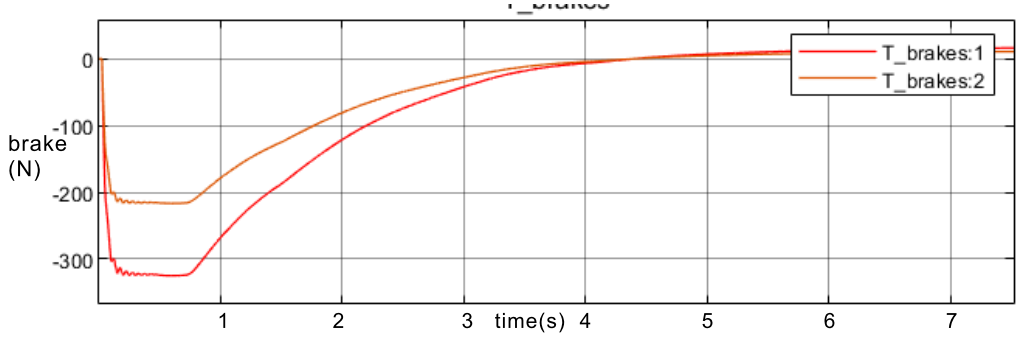


(c) Lateral acceleration-70 km/h

Figure 4.6: Vehicle speed, lateral acceleration and sideslip angle responses during the emergency steering manoeuvre for initial vehicle speeds 70km/hr.

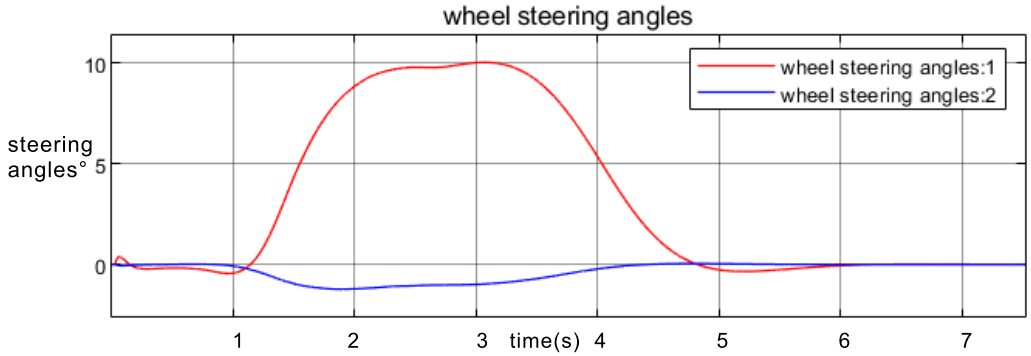


(a) Front and Rear steering angles-60 km/h

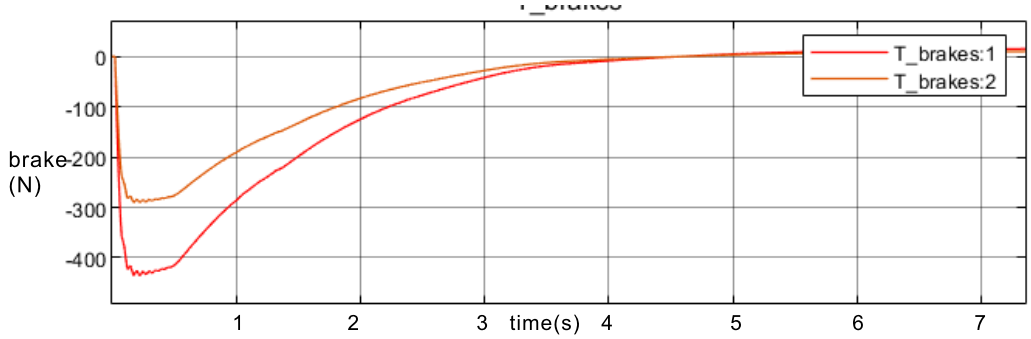


(b) Front and Rear braking-60 km/h

Figure 4.7: Steering angles and braking responses during the emergency manoeuvre manoeuvre for initial vehicle speeds 60km/hr.

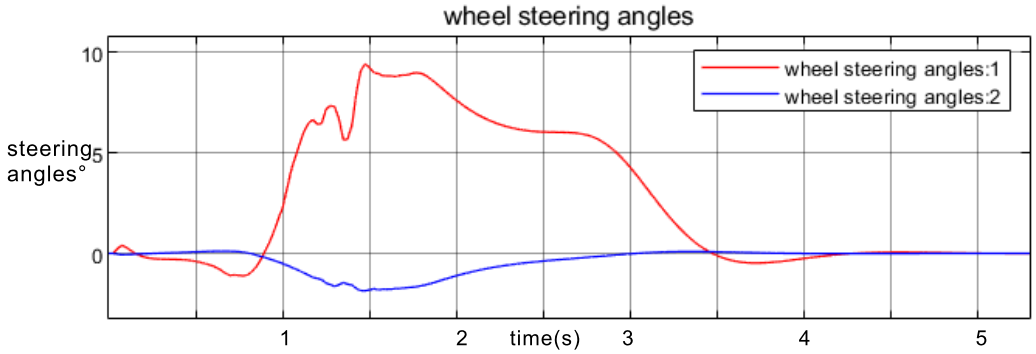


(a) Front and Rear steering angles-65 km/h

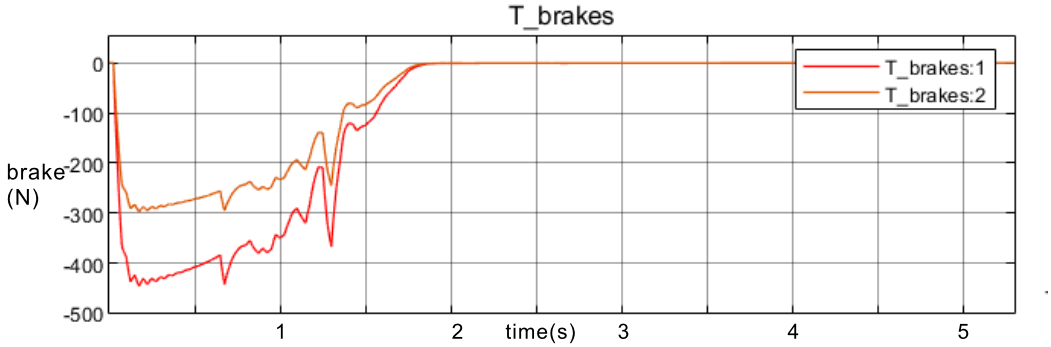


(b) Front and Rear braking-65 km/h

Figure 4.8: Steering angles and braking responses during the emergency manoeuvre manoeuvre for initial vehicle speeds 65km/hr.



(a) Front and Rear steering angles-70 km/h



(b) Front and Rear braking-70 km/h

Figure 4.9: Steering angles and braking responses during the emergency manoeuvre manoeuvre for initial vehicle speeds 70km/hr.

ing angle, rear steering angle, and braking torque applied throughout the simulation.

The front steering angle represents the primary mechanism used by the controller to follow the reference trajectory. As the vehicle approaches the curved section of the path, the front steering command increases progressively and reaches a maximum value of approximately 10°. This steering action enables the vehicle to negotiate the turn while maintaining a small tracking error. Following completion of the manoeuvre, the steering angle gradually returns to zero as the vehicle transitions back to straight-line motion.

In contrast, the rear steering angle remains significantly smaller, reaching a maximum magnitude of approximately 1°. The rear axle therefore acts primarily as a stabilizing actuator rather than a path-generation actuator. By introducing small rear-wheel steering corrections, the controller improves vehicle yaw response and enhances lateral stability during the transient phase of the manoeuvre.

The braking torque exhibits a sharp increase at the beginning of the manoeuvre, reaching a peak value of approximately 400 Nm for fron wheels and 290 Nm for rear wheels. This aggressive initial braking action reduces the vehicle speed before entering the most demanding section of the path, thereby decreasing the required lateral tyre forces and improving overall stability. As the manoeuvre progresses, the braking demand gradually decreases and approaches zero once the vehicle has completed the turn.

The braking effort is distributed between the front and rear axles using a fixed 60/40 brake distribution ratio. Consequently, 60% of the braking torque is applied to the front axle while the remaining 40% is assigned to the rear axle. This configuration reflects conventional automotive braking systems and takes advantage of the forward load transfer occurring during deceleration. The larger braking contribution at the front axle improves vehicle stability and reduces the likelihood of rear-wheel lockup.

Overall, the control actions demonstrate that the NMPC controller effectively coordinates steering and braking inputs to satisfy the path-tracking objective while maintaining stable vehicle behaviour throughout the manoeuvre.

4.5 Constraint Satisfaction

An important requirement of any NMPC-based controller is the ability to satisfy system constraints while simultaneously achieving the control objective. In the proposed framework, constraints were imposed on the vehicle states, wheel rotational speeds, steering actuators, braking actuator, and tyre slip

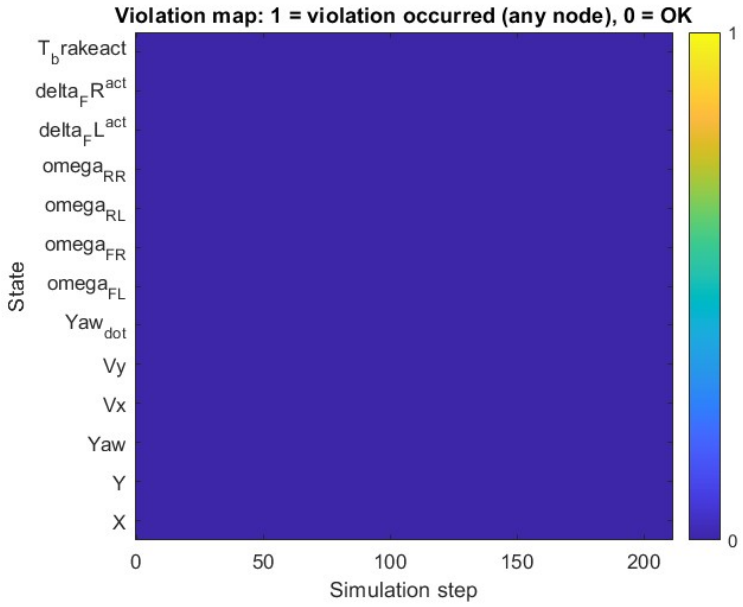


Figure 4.10: Constraint violation map for all constrained states during the evasive manoeuvre. A value of zero indicates that all constraints are satisfied.

ratios. These limits were introduced to ensure physically realistic and safe vehicle operation throughout the manoeuvre.

Figure 4.10 presents the constraint violation map obtained during the simulation. The horizontal axis represents the simulation step, while the vertical axis corresponds to the constrained system states. A value of one indicates that at least one violation occurred at the corresponding simulation instant, whereas a value of zero indicates full constraint satisfaction.

As shown in Figure 4.10, all entries remain equal to zero throughout the entire simulation. No violations were detected for any of the constrained states, including vehicle velocity, lateral velocity, yaw rate, wheel rotational speeds, steering actuator states, or braking actuator states.

These results demonstrate that the proposed NMPC controller successfully maintains feasibility while executing the evasive manoeuvre. The optimization algorithm continuously generates admissible control actions that satisfy the imposed physical limitations of the vehicle model. This behaviour is particularly important during aggressive manoeuvres, where large steering and braking commands could otherwise push the system beyond its operational limits.

The absence of state constraint violations confirms that the controller preserves safe operating conditions throughout the manoeuvre while main-

taining the desired path-tracking performance.

4.6 Tyre Slip Behaviour

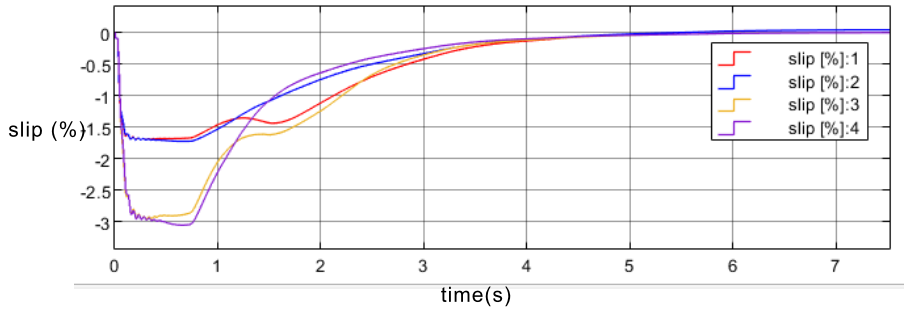


Figure 4.11: Tyre slip behaviour at 60km/hr.

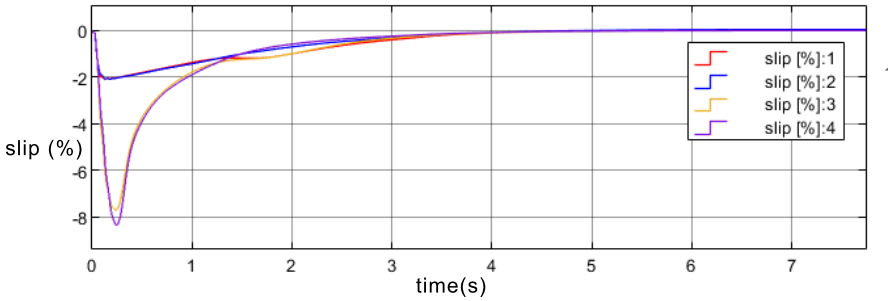


Figure 4.12: Tyre slip behaviour at 65km/hr.

The longitudinal slip ratio is one of the most important variables governing tyre force generation and vehicle stability. Excessive wheel slip can reduce the available tyre-road friction and may lead to loss of vehicle control, particularly during aggressive braking manoeuvres. For this reason, longitudinal tyre slips were included as soft constraints within the NMPC formulation.

Figure 4.11,Figure 4.12 and Figure 4.13 presents the evolution of the longitudinal slip ratios for all four wheels during the evasive manoeuvre. Negative slip values indicate braking conditions, while positive values correspond to driving or traction conditions.

At the beginning of the manoeuvre, the controller commands a significant braking action, resulting in an increase in braking slip at all four wheels. The largest slip magnitude is observed at the rear-left wheel, which reaches approximately -3% for 60km/hr, -8% for 65km/hr and -15% for 70km/hr as the braking efforts and tyre locking are more prone to happen in 70km/hr.

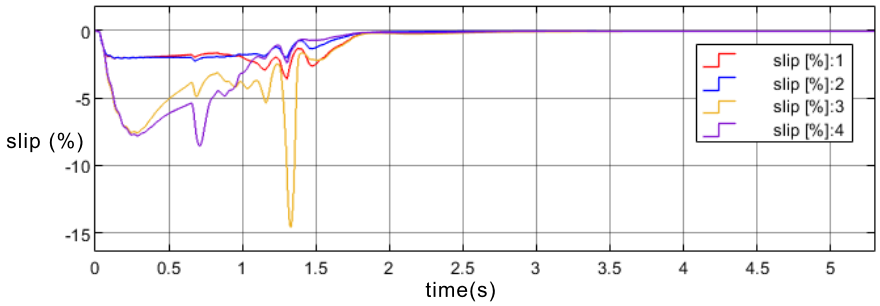


Figure 4.13: Tyre slip behaviour at 70km/hr.

The remaining wheels exhibit smaller peak slip values but follow a similar overall trend.

As the vehicle speed decreases and the braking demand is progressively reduced, the slip ratios gradually converge toward zero. This behaviour indicates that the wheels return to near pure rolling conditions after the most demanding phase of the manoeuvre has been completed.

The smooth evolution of the slip ratios demonstrates that the NMPC controller successfully regulates wheel slip while generating the braking forces required for path tracking and vehicle stabilization. Furthermore, no abrupt oscillations or divergence are observed, indicating stable tyre-force generation throughout the simulation.

The results also confirm the effectiveness of the adopted soft-constraint formulation. Although moderate slip levels are temporarily permitted to maximize braking performance, the controller prevents excessive wheel slip and maintains the tyres within a physically realistic operating region.

4.7 NMPC Prediction Behaviour

The internal predictions generated by the NMPC controller provide valuable information regarding the evolution of the optimization process and the anticipated vehicle response. At each sampling instant, the controller predicts future state trajectories, wheel rotational speeds, and control actions over the prediction horizon before applying only the first control input.

To evaluate the influence of increasing vehicle speed on the prediction quality, the predicted trajectories obtained at initial speeds of 60 km/h, 65 km/h, and 70 km/h are compared. The resulting prediction maps illustrate how the controller adapts its future plans as the manoeuvre becomes progressively more demanding.

4.7.1 Predicted Vehicle States

Figure 4.14 compares the predicted vehicle-state trajectories generated by the NMPC controller at different initial vehicle speeds.

At 60 km/h, the prediction horizon exhibits smooth and well-behaved trajectories. The predicted longitudinal velocity decreases monotonically due to braking, while the lateral velocity and yaw-rate states increase gradually during the cornering phase before returning toward zero as the vehicle exits the curve.

At 65 km/h, the same overall behaviour is observed; however, small oscillations begin to appear in several predicted states, particularly in the lateral velocity and longitudinal velocity predictions. These oscillations occur during the most demanding portion of the manoeuvre and indicate increased controller activity required to satisfy the path-tracking objective.

At 70 km/h, the prediction horizon becomes noticeably more complex. The predicted velocity and lateral-dynamics states exhibit stronger oscillatory behaviour, reflecting the increased difficulty of simultaneously maintaining path tracking, stability, and constraint satisfaction at higher speeds. Despite these oscillations, the predicted trajectories remain bounded and converge toward physically realistic solutions.

The results indicate that the NMPC controller remains capable of generating feasible future trajectories even as the operating conditions approach the limits of the manoeuvre.

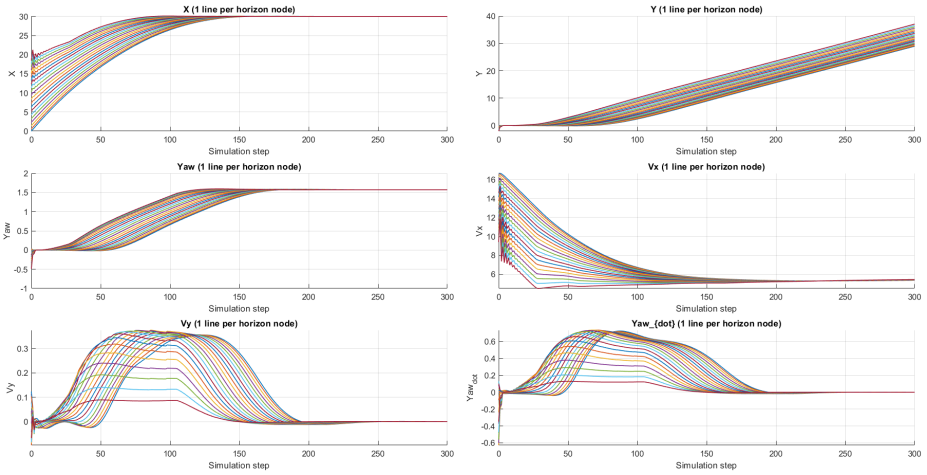
4.7.2 Predicted Wheel Rotational Speeds

Figure 4.15 compares the wheel-speed predictions obtained at the three investigated vehicle speeds.

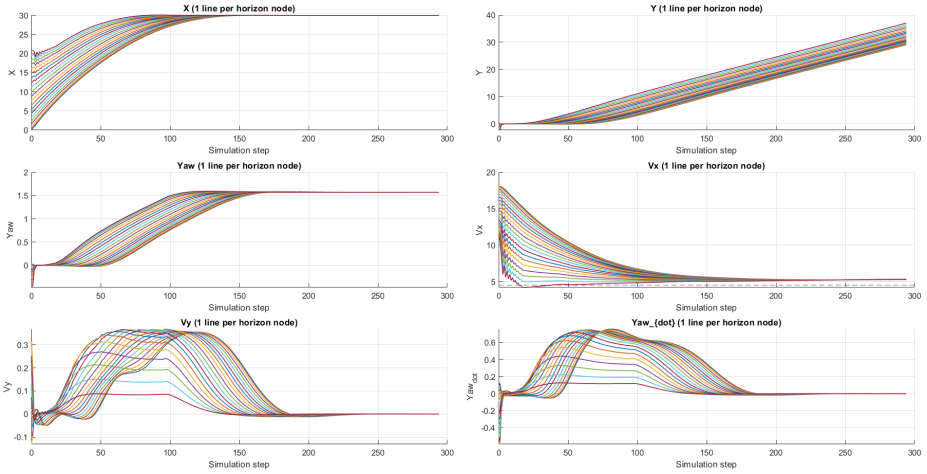
At 60 km/h, the predicted wheel rotational speeds decrease smoothly throughout the horizon and converge toward the final steady-state value with minimal oscillation.

At 65 km/h, transient disturbances begin to appear in the wheel-speed predictions during the cornering phase. Small oscillations are observed as the controller coordinates braking and steering actions while maintaining vehicle stability.

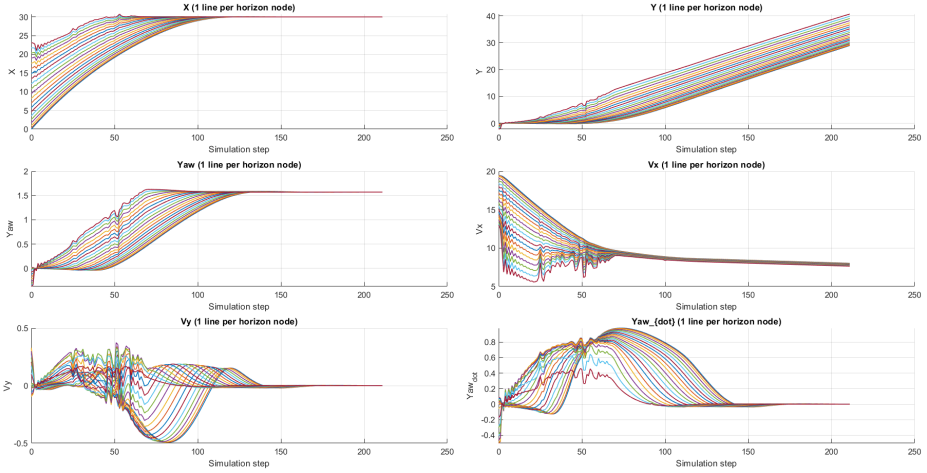
The most pronounced behaviour is observed at 70 km/h, where significant fluctuations appear in all wheel-speed predictions during the most aggressive portion of the manoeuvre. These oscillations indicate that the tyre forces are approaching the limits of the available tyre-road friction. Nevertheless, the predicted wheel speeds remain bounded and eventually converge toward the expected operating condition.



(a) Prediction States-60 km/h

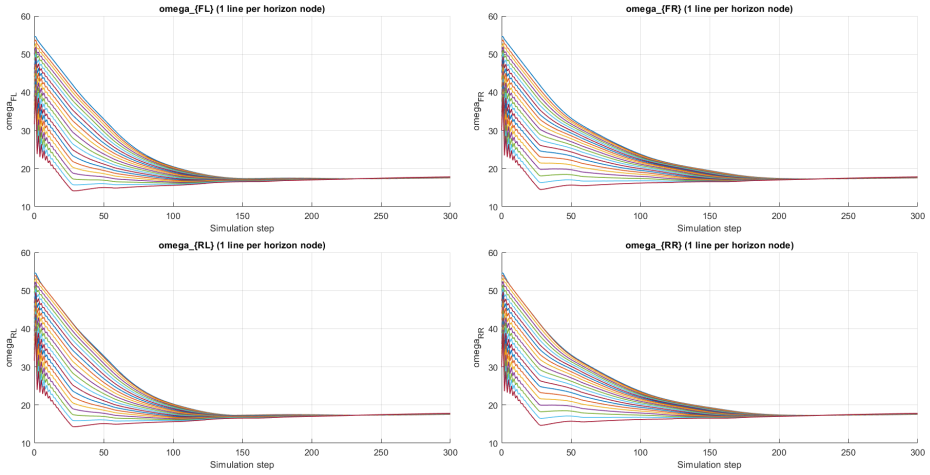


(b) Prediction States-65 km/h

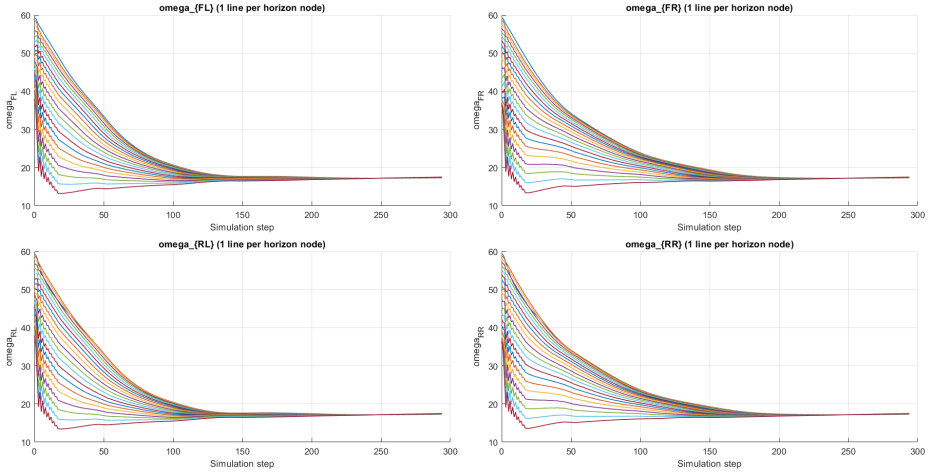


(c) Prediction States-70 km/h

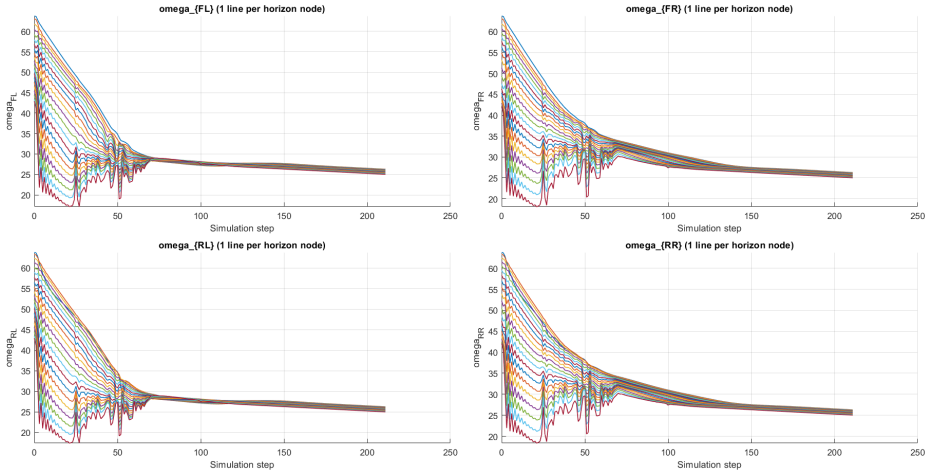
Figure 4.14: Prediction Vehicle States at different initial speeds.



(a) Prediction Wheel Rotation-60 km/h



(b) Prediction Wheel Rotation-65 km/h



(c) Prediction Wheel Rotation-70 km/h

Figure 4.15: Prediction Wheel Rotation at different initial speeds.

The wheel-speed prediction maps therefore reveal the increasing dynamic complexity encountered by the controller as vehicle speed increases.

4.7.3 Predicted Control Inputs

Figure 4.16 presents the predicted steering and braking actions generated by the NMPC controller at different vehicle speeds.

For the 60 km/h case, the control predictions are smooth and exhibit a clear structure. The front steering angle gradually increases during the turning phase, while the braking torque decreases smoothly after the initial deceleration demand.

At 65 km/h, additional corrective actions become visible. Small oscillations appear in the steering and braking predictions as the controller compensates for the increased vehicle inertia and larger tyre-force requirements.

At 70 km/h, the control activity increases substantially. Oscillatory behaviour appears in both the steering commands and braking torque predictions, particularly during the transition into the curved segment of the path. These oscillations indicate repeated replanning by the optimizer as it seeks a feasible solution while simultaneously satisfying the tracking objective and the imposed constraints.

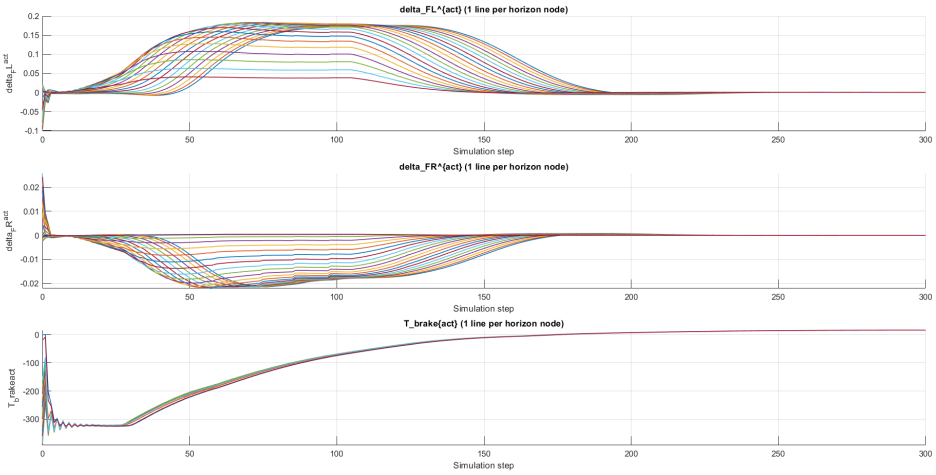
Although the control effort becomes more aggressive at higher speeds, the controller remains capable of generating admissible steering and braking commands throughout the manoeuvre. The predictions eventually converge as the vehicle exits the curve and returns to a stable operating condition.

4.8 Constraint Satisfaction and Solver Performance

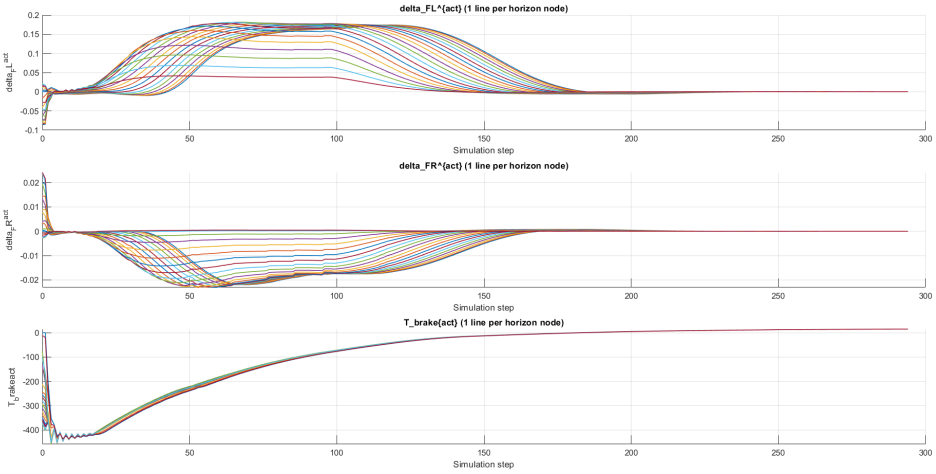
An important requirement of the proposed NMPC controller is the ability to generate dynamically feasible control actions while satisfying all imposed state, actuator and tyre constraints throughout the manoeuvre.

Figure XX presents the constraint violation map generated during the simulation. Each row corresponds to one system state or actuator variable, while each column represents a simulation step. A value of one indicates that at least one prediction node violated the corresponding constraint, whereas a value of zero indicates successful constraint satisfaction.

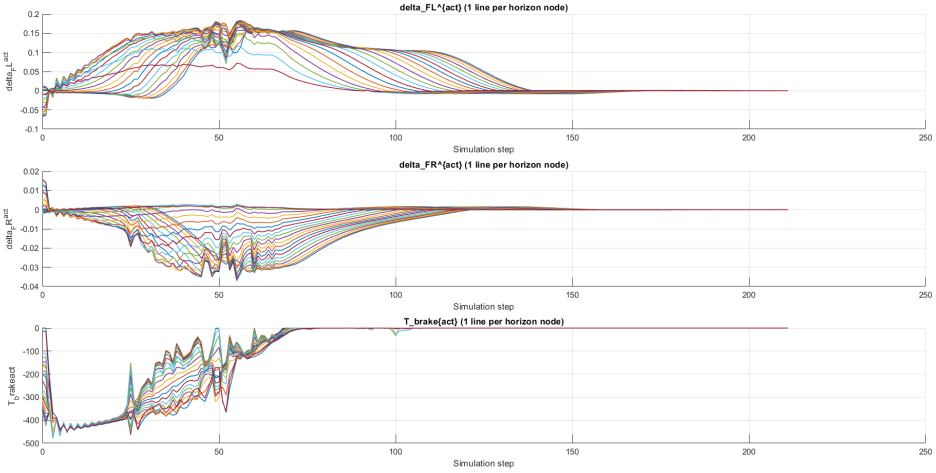
The results show that no constraint violations occurred during the complete simulation horizon. All state variables remained within their prescribed limits, including vehicle velocity, lateral velocity, yaw rate, wheel angular velocities, steering actuator states and braking actuator states. This confirms



(a) Prediction Control Inputs-60 km/h



(b) Prediction Control Inputs-65 km/h



(c) Prediction Control Inputs-70 km/h

Figure 4.16: Prediction Control Inputs at different initial speeds.

that the NMPC formulation successfully maintained feasibility while performing the emergency manoeuvre.

In addition to state constraints, longitudinal tyre slip constraints were introduced as soft constraints to prevent excessive wheel lock and preserve tyre force generation. The slip ratio responses for all four wheels remained within the admissible operating region throughout the manoeuvre. Although temporary increases in slip occurred during the initial braking phase, the controller quickly regulated the wheel dynamics and returned the slip values towards zero as the vehicle approached the end of the manoeuvre.

Solver convergence was evaluated using the ACADOS SQP iteration history and solver status indicators. The solver status remained equal to zero during the entire simulation, indicating successful optimization convergence at every sampling instant for all investigated vehicle speeds. The SQP iteration history provides additional insight into the computational effort required by the nonlinear optimization problem. For the 60 km/h and 65 km/h manoeuvres, the solver converged with relatively low iteration counts throughout the simulation. In contrast, the 70 km/h case exhibited a significant increase in SQP iterations during the entry into the curved section of the trajectory. This behaviour indicates that the optimization problem became considerably more challenging as vehicle speed increased and the controller was required to simultaneously coordinate aggressive steering and braking actions while satisfying the imposed constraints. Despite this increase in computational effort, the solver maintained successful convergence at every sampling instant, demonstrating the robustness of the ACADOS-based NMPC implementation under demanding operating conditions.

These results demonstrate that the proposed ACADOS-based NMPC implementation provides reliable real-time optimization performance while maintaining constraint satisfaction and numerical stability under aggressive vehicle operating conditions.

4.9 Chapter Summary

This chapter presented the simulation results obtained from the proposed ACADOS-based Nonlinear Model Predictive Control framework for autonomous emergency manoeuvre execution. The controller was evaluated on a combined straight-line and curved reference path at initial vehicle speeds of 60 km/h, 65 km/h and 70 km/h.

The trajectory tracking results demonstrated that the controller successfully guided the vehicle along the reference path for all investigated operating conditions. The cross-track and heading errors remained small through-

out the manoeuvre, indicating accurate path-following performance despite the simultaneous steering and braking actions required during the transient phase.

The evolution of the control inputs showed that the NMPC controller effectively coordinated front steering, rear steering and braking torque to achieve the desired vehicle motion. The implemented 60/40 front-to-rear brake torque distribution contributed to stable deceleration while maintaining adequate vehicle controllability throughout the manoeuvre.

Analysis of the vehicle dynamic states confirmed that the controller maintained stable longitudinal, lateral and yaw dynamics. Although increasing vehicle speed resulted in larger lateral velocity, yaw rate and sideslip responses, the vehicle remained controllable and successfully completed the manoeuvre without loss of stability.

The prediction horizon analysis provided additional insight into the operation of the NMPC algorithm. The predicted state and control trajectories evolved smoothly along the horizon and consistently converged toward the desired reference path, demonstrating the controller's ability to anticipate future vehicle behaviour and generate proactive control actions.

Constraint satisfaction analysis verified that all imposed state and actuator limits were respected during the complete simulation. Furthermore, the tyre slip constraints remained within acceptable bounds, preventing excessive wheel lock and preserving tyre force generation. Solver statistics showed successful convergence of the ACADOS optimization routine at every sampling instant, confirming the numerical robustness and real-time suitability of the proposed implementation.An increase in vehicle speed from 60 km/h to 70 km/h resulted not only in larger vehicle dynamic responses but also in increased optimization effort. This effect is reflected in the SQP iteration history, where the 70 km/h scenario required substantially more iterations during the most demanding phase of the manoeuvre. The observation highlights the growing nonlinearity of the control problem as the vehicle approaches more aggressive operating conditions.

Overall, the simulation results demonstrate that the proposed nonlinear model predictive controller provides accurate trajectory tracking, stable vehicle dynamics, effective control coordination and reliable constraint handling over a range of demanding operating conditions. These findings validate the suitability of the developed framework for autonomous emergency manoeuvre applications and establish a foundation for future extensions involving more complex vehicle models, obstacle avoidance scenarios and experimental validation.

Chapter 5

Conclusions and Future Work

5.1 Conclusions

This thesis presented the development and implementation of a Nonlinear Model Predictive Control (NMPC) framework for autonomous vehicle trajectory tracking during high-demand emergency manoeuvres. The controller was formulated using a nonlinear vehicle model incorporating longitudinal, lateral and yaw dynamics together with wheel rotational dynamics, steering actuator dynamics and braking actuator dynamics. The resulting optimal control problem was solved using the ACADOS optimization framework, enabling efficient real-time implementation.

A reference path consisting of a straight segment, a constant-radius curve and a final straight segment was used to evaluate the controller under challenging transient conditions. The proposed NMPC formulation simultaneously optimized front steering, rear steering and braking torque while accounting for vehicle dynamics, actuator limitations and tyre slip constraints.

Simulation studies were conducted at initial vehicle speeds of 60 km/h, 65 km/h and 70 km/h. The results demonstrated that the controller successfully tracked the reference trajectory in all investigated scenarios while maintaining vehicle stability throughout the manoeuvre. Cross-track and heading errors remained small, indicating accurate path-following performance even during the most demanding portions of the trajectory.

The coordinated control strategy generated smooth steering and braking actions while respecting the implemented actuator constraints. The braking system employed a 60/40 front-to-rear brake torque distribution, providing stable vehicle deceleration and contributing to the overall controllability of the vehicle during the manoeuvre.

Analysis of the vehicle dynamic responses showed that increases in ve-

hicle speed resulted in larger lateral velocity, yaw rate and sideslip angle responses. Nevertheless, the controller maintained stable behaviour and successfully completed the manoeuvre without loss of control. Constraint monitoring confirmed that all state and actuator limits remained satisfied throughout the simulations, while the soft tyre slip constraints effectively prevented excessive wheel slip.

The prediction horizon analysis further demonstrated the predictive capabilities of the NMPC formulation. Predicted state and control trajectories evolved consistently toward the desired path, illustrating the controller's ability to anticipate future vehicle behaviour and generate proactive control actions.

Overall, the obtained results confirm that the proposed ACADOS-based NMPC framework is capable of providing accurate trajectory tracking, stable vehicle dynamics and reliable constraint handling during aggressive emergency manoeuvres. The study demonstrates the potential of nonlinear predictive control techniques for advanced autonomous vehicle applications requiring high levels of safety and dynamic performance.

5.2 Main Contributions

The main contributions of this thesis can be summarized as follows:

1. **Development of a nonlinear vehicle dynamics model for predictive control applications**

   A nonlinear vehicle model was developed to capture the longitudinal, lateral and yaw dynamics of the vehicle together with wheel rotational dynamics, steering actuator dynamics and braking actuator dynamics. The model incorporated nonlinear tyre behaviour through a reduced Pacejka Magic Formula tyre model, enabling realistic representation of tyre force generation during aggressive manoeuvres.

2. **Formulation of an ACADOS-based nonlinear model predictive controller**

   A nonlinear model predictive control framework was formulated using the developed vehicle model. The optimal control problem was implemented within the ACADOS environment, allowing efficient real-time solution of the nonlinear optimization problem. The controller simultaneously optimized front steering, rear steering and braking torque while accounting for system dynamics, actuator limitations and tyre slip constraints.

3. **Integrated vehicle stabilization through coordinated steering and braking control**

   Unlike conventional path-following approaches that rely solely on steering control, the proposed framework coordinated front steering, rear steering and braking actions within a unified optimization problem. This integrated approach improved vehicle stability during transient manoeuvres and enabled successful trajectory tracking under demanding operating conditions.

4. **Validation under high-speed emergency manoeuvre scenarios**

   The proposed controller was evaluated through simulation studies at initial vehicle speeds of 60 km/h, 65 km/h and 70 km/h. The results demonstrated accurate trajectory tracking, stable vehicle behaviour and successful constraint satisfaction across all investigated scenarios. Furthermore, the analysis of prediction horizons and solver performance provided additional insight into the behaviour and computational feasibility of the implemented NMPC framework.

5.3 Limitations

Although the proposed NMPC framework demonstrated satisfactory performance during the investigated emergency manoeuvres, several limitations should be acknowledged.

First, the study was conducted entyrely within a simulation environment. While the vehicle model captures the dominant longitudinal, lateral and yaw dynamics, real-world vehicles are subject to additional uncertainties such as sensor noise, actuator delays, parameter variations and external disturbances. Consequently, experimental validation using a physical vehicle or a hardware-in-the-loop platform is required to fully assess the practical applicability of the controller.

Second, the tyre behaviour was represented using a reduced Pacejka Magic Formula tyre model. Although this model provides an accurate approximation of tyre force generation over a wide operating range, it does not capture all aspects of tyre dynamics, including transient relaxation effects, temperature variations, road surface irregularities and changes in tyre characteristics due to wear.

Third, the emergency manoeuvre investigated in this work was performed on a predefined reference path consisting of straight and curved segments. The controller therefore focused on trajectory tracking rather than real-time

trajectory generation or obstacle avoidance. In practical autonomous driving applications, the path-following controller would typically operate together with a higher-level motion-planning module responsible for generating collision-free trajectories in dynamic environments.

Fourth, the road conditions considered in this study assumed a uniform tyre-road friction coefficient. Variations in road friction resulting from wet, icy or otherwise degraded surfaces were not investigated. Such conditions could significantly influence vehicle behaviour and may require additional adaptation mechanisms within the controller.

Finally, the computational performance was evaluated using the selected prediction horizon, sampling time and solver configuration. Although successful real-time execution was achieved within the simulation framework, different vehicle models, longer prediction horizons or more complex driving scenarios may lead to increased computational requirements and warrant further optimization.

Despite these limitations, the developed framework provides a valuable platform for investigating nonlinear predictive control strategies for autonomous vehicle applications and establishes a solid foundation for future research and development.

5.4 Future Research Directions

The results obtained in this thesis demonstrate the effectiveness of nonlinear model predictive control for autonomous vehicle trajectory tracking during high-demand manoeuvres. Nevertheless, several opportunities exist for extending and improving the proposed framework.

A natural continuation of this work is the experimental validation of the controller on a real vehicle or a hardware-in-the-loop platform. Such validation would enable assessment of the controller under realistic operating conditions, including sensor noise, actuator delays, model uncertainties and external disturbances that are difficult to reproduce accurately in simulation.

Another important extension involves the integration of a higher-level motion-planning module. In the present study, the controller followed a predefined reference trajectory. Future developments could combine the NMPC framework with real-time trajectory generation and obstacle avoidance algorithms, enabling the vehicle to autonomously react to dynamic traffic scenarios and unexpected obstacles.

The vehicle model could also be enhanced by incorporating additional dynamics, such as roll, pitch and load-transfer effects. While the current model captures the dominant planar vehicle dynamics, a higher-fidelity rep-

resentation would improve prediction accuracy under extreme manoeuvring conditions and provide a more realistic description of vehicle behaviour near the handling limits.

Further research may also investigate the controller's performance under varying road and environmental conditions. Simulations involving different tyre-road friction coefficients, wet or icy surfaces, and changing road conditions would provide a more comprehensive evaluation of controller robustness and adaptability.

From a computational perspective, alternative NMPC formulations and solver configurations may be explored to further reduce computational effort and improve scalability. This would be particularly beneficial for applications involving longer prediction horizons, more detailed vehicle models or complex traffic environments.

Finally, recent advances in machine learning and artificial intelligence offer promising opportunities for enhancing predictive control frameworks. Data-driven models, neural-network-based vehicle representations and learning-assisted prediction techniques could be integrated with the NMPC architecture to improve model accuracy, reduce computational complexity and increase adaptability to varying driving conditions. Such hybrid approaches represent an active area of research in autonomous vehicle control and may provide significant performance improvements in future implementations.

Bibliography

[1] J. Funke, M. Brown, S. Erlien, and J. C. Gerdes, "Collision avoidance and stabilization for autonomous vehicles in emergency scenarios," *IEEE Transactions on Control Systems Technology*, vol. 25, no. 4, pp. 1204–1216, 2017.

[2] T. P. Weber and J. C. Gerdes, "Modeling and control for dynamic drifting trajectories," *IEEE Transactions on Intelligent Vehicles*, vol. 9, no. 2, pp. 3731–3745, 2024.

[3] J. Y. M. Goh, M. Thompson, J. Dallas, and A. Balachandran, "Beyond the stable handling limits: Nonlinear model predictive control for highly transient autonomous drifting," *Vehicle System Dynamics*, vol. 62, no. 10, pp. 2590–2613, 2024.

[4] R. Rajamani, *Vehicle Dynamics and Control*, 2nd ed. Springer, 2012.

[5] B. Paden, M. Cap, S. Z. Yong, D. Yershov, and E. Frazzoli, "A survey of motion planning and control techniques for self-driving urban vehicles," *IEEE Transactions on Intelligent Vehicles*, vol. 1, no. 1, pp. 33–55, 2016.

[6] L. Grüne and J. Pannek, *Nonlinear Model Predictive Control*, 2nd ed. Springer, 2017.

[7] Z. Wang *et al.*, "Enhanced active safety through integrated autonomous drifting and direct yaw moment control via nonlinear model predictive control," *Applied Sciences*, vol. 11, no. 6373, 2021.

[8] Author, "A torque vectoring control for enhancing vehicle performance," *Vehicle System Dynamics*, 2023.

[9] G. Zhu and W. Hong, "Nmpc-based path tracking control through cascaded discretization method considering handling stability for 4ws autonomous vehicles under extreme conditions," *World Electric Vehicle Journal*, vol. 15, no. 12, p. 573, 2024.

[10] H. B. Pacejka, *Tyre and Vehicle Dynamics*, 3rd ed. Oxford, UK: Butterworth-Heinemann, 2012.

[11] R. Verschueren *et al.*, "acados: a modular open-source framework for fast embedded optimal control," *Mathematical Programming Computation*, 2021.